Check for updates

Received: 7 June 2023 | Revised: 31 January 2024 | Accepted: 5 March 2024

DOI: 10.1002/zamm.202300432

ORIGINAL PAPER

An alternative approach to averaging in nonlinear systems using classical probability density

Attila Genda[1,3] | **Alexander Fidlin**[1] | **Oleg Gendelman**[2]

[1]Institute of Engineering Mechanics, Karlsruhe Institute of Technology, Karlsruhe, Germany

[2]Mechanical Engineering, Technion—Israel Institute of Technology, Haifa, Israel

[3] Building 10.23, 1st floor, Room 101, Kaiserstr. 10, Karlsruhe, Germany

Correspondence
Attila Genda, Institute of Engineering Mechanics, Karlsruhe Institute of Technology, Karlsruhe, Germany.
Email: attila.genda@kit.edu

Present address
Attila Genda, Building 10.23, 1st floor, Room 101, Kaiserstr. 10, Karlsruhe, Germany

Funding information
Deutsche Forschungsgemeinschaft, Grant/Award Number: 508244284

The averaging method is a widely used technique in the field of nonlinear differential equations for effectively reducing systems with "fast" oscillations overlaying "slow" drift. The method involves calculating an integral, which can be straightforward in some cases but can also require simplifications such as series expansions. We propose an alternative approach that relies on the classical probability density (CPD) of the "fast" variable. Furthermore, we demonstrate the equivalence between the averaging integral and the cross-correlation product of the CPD and the target function. This equivalence simplifies handling many problems, particularly those involving piecewise-defined target functions. We propose an effective numerical method to calculate the averaged function, taking advantage of the well-known mathematical properties of cross-correlation products.

1 | INTRODUCTION

The averaging method is widely used in nonlinear differential equations to reduce complex systems with "fast" oscillations and "slow" drifts. It is an essential tool for analyzing and synthesizing such systems, as it enables the effective representation of the underlying dynamics. The technique has been extensively studied and applied in various fields, including physics [1–4], engineering [5–8], and biology [9].

The basic idea behind the averaging method is to transform a rapidly oscillating system into a slowly varying one, maintaining the significant properties of the original one. Then, the averaged system can give more analytic insight into the system's "slow" dynamics or might reduce computational costs. The simplification is achieved by calculating the time average of the rapidly oscillating variables over a period of the "fast" motion.

Although the idea of averaging is much older and has been used many years before, in 1934 *Krylov and Bogulyubov* developed first a general averaging approach and showed that the solution of the averaged system approximates the exact dynamics [10, 11]. A historical overview of the works of Krylov, Bogulyubov, and Mitropolsky can be found in Ref. [12].

Over the past few decades, the averaging method has been the subject of numerous studies, and various approaches have been proposed to address its limitations and improve its accuracy. For example, in Ref. [13], the author proposed modifying

This is an open access article under the terms of the Creative Commons Attribution-NonCommercial License, which permits use, distribution and reproduction in any medium, provided the original work is properly cited and is not used for commercial purposes.
© 2024 The Authors. *ZAMM - Journal of Applied Mathematics and Mechanics* published by Wiley-VCH GmbH.

the classical averaging method that accounts for higher-order terms in the expansion. The averaging technique has also been applied in stochastic differential equations [14]: a stochastic averaging method for studying the effects of time-delayed feedback control on quasi-integrable Hamiltonian systems subjected to Gaussian white noise was proposed in Ref. [15]. In Ref. [16], the authors proposed a stochastic averaging technique to analyze randomly excited single-degree-of-freedom (SDOF) strongly nonlinear systems with delayed feedback fractional-order proportional-derivative (PD) control.

The growth of the knowledge on the averaging method resulted in the publication of numerous articles [17–19], book chapters [20–22], and comprehensive monographs such as *Averaging Methods in Nonlinear Dynamical Systems* [23] and *Nonlinear oscillations in mechanical engineering* [24]. These works offer an in-depth look at the theory and practical applications of the averaging method in various areas of study.

In addition, the averaging method has also been applied to various real-world problems, including the analysis of power electronic systems [25, 26] and the study of climate dynamics [27].

Parallel to its analytic applications, the averaging method also finds its numerical applications [28]. In Ref. [29] *Leimkuhler and Reich* described a reversible staggered time-stepping method for simulating long-term dynamics formulated on two or more time scales.

These examples demonstrate the versatility and importance of the averaging method in studying nonlinear differential equations. Despite its numerous applications and improvements, the method still presents many challenges and opportunities for further research.

Although calculating the averaging integral is typically straightforward, obtaining an analytic expression can pose algebraic difficulties in many cases. Additionally, there may be a need to perform averaging using numerical or experimental data. Traditional quadrature methods for averaging require time series data, which can be particularly challenging to obtain for "fast" motions. However, measuring the probability of finding a particle at a specific position can often be a more accessible approach. For example, a camera with a sufficiently long exposure time can generate an image with a pixel brightness proportional to the CPD.

In the present paper, an alternative formula, based on results regarding the Lebesgue integral [30], is proposed to evaluate the averaging integral for the case of a dependent variable that can be decomposed into the sum of a "fast" motion and a "slow" drift. We show that the averaging integral is equivalent to the cross-correlation of the "fast" motion's CPD and the original function subjected to averaging. In general, the average of the function is not necessarily equal to the function of the average.

The CPD is a well-known concept in classical and quantum mechanics [31] describing the probability that a particle, following a certain motion, can be found at a given position. For simple periodic motions, the CPD can be derived analytically [32–34]. However, the evaluation is often possible numerically only for more complex motions.

In the following, we will interchangeably use the terms probability density function (PDF) and CPD since their mathematical properties are identical.

The paper is structured as follows: in Section 2, the equivalence of the averaging integral and the CPD-based cross-correlation of the target function is proven, followed by some important implications on the efficient calculation and properties of the averaged function. In Section 3, the CPDs of several types of oscillations are derived. In Section 4, different methods are described for the efficient numerical calculation of CPDs and the averaged function itself. Section 5 summarizes the results of the article and provides scope for applications and further research of the cross-correlation-based averaging method. The Appendix contains additional information on the moments and partial moments of various CPDs relevant to engineering applications.

2 | THEOREM ON CROSS-CORRELATION-BASED AVERAGING

To alternatively calculate the averaging integral, we consider the following theorem regarding the change of variables in Lebesgue integrals. The text is adapted from Ref. [30].

Definition 1. Given a measure space $(X, \mathcal{A}, \mu)$, and a σ-algebra $\mathcal{B}$ on a set Y, consider a mapping $\phi : X \to Y$ that satisfies $\phi^{-1}(B) \in \mathcal{A}$ for every $B \in \mathcal{B}$. For a measurable function $\rho : X \to [0, \infty)$, we define a new function $\nu : \mathcal{B} \to \mathbb{R}$ as follows:

$$\nu(B) = \int_{\phi^{-1}(B)} \rho(x)\, d\mu(x), \quad B \in \mathcal{B}. \tag{1}$$

15214001, 0, Downloaded from https://onlinelibrary.wiley.com/doi/10.1002/zamm.202300432, Wiley Online Library on [23/03/2024]. See the Terms and Conditions (https://onlinelibrary.wiley.com/terms-and-conditions) on Wiley Online Library for rules of use; OA articles are governed by the applicable Creative Commons License

ν is a measure on $\mathcal{B}$, called the *weighted image* of μ by ρ through ϕ, with ρ called the *weight function*. This construction does not presuppose ϕ to be injective or surjective.

The following theorem asserts the transference of integration through ϕ under the influence of ρ.

Theorem 1. *For the ρ-weighted image ν of a measure μ by a map $\phi : X \to Y$, every non-negative measurable function f on Y, when composed with ϕ, remains measurable. Furthermore, for such functions, the integrals over Y with respect to ν and over X with respect to μ are equivalent:*

$$\int_Y f(y)\, d\nu(y) = \int_X f(\phi(x))\omega(x)\, d\mu(x). \tag{2}$$

This equivalence extends to all summable functions f on Y.

The adapted text ends here. We refer the reader to Ref. [30] for a proof of the theorem. In the following, we demonstrate how the weight function ρ can be obtained to evaluate the classical averaging integral in an alternative manner.

Definition 2. Let $g_i : (a, b) \to \mathbb{R}$ be either a strictly monotonically increasing C^1 function with the parameter $d_i = 0$ when the sign of its derivative is positive or a strictly monotonically decreasing C^1 function with the parameter $d_i = 1$ when the sign of its derivative is negative. Then, its CPD is defined [35] by

$$\rho_i : \begin{cases} \mathbb{R} & \to \mathbb{R}^{0+} \\ x & \mapsto \frac{(-1)^{d_i}}{g_i'[g_i^{-1}(x)]} \frac{1}{b-a} \mathbf{1}_{(g_i(a), g_i(b))}(x), \end{cases} \tag{3}$$

where slightly abusing the notation (during the whole article) to set the value of ρ_i to 0 outside $(g_i(a), g_i(b))$, we use the indicator function defined as

$$\mathbf{1}_X(x) = \begin{cases} 1 & x \in X, \\ 0 & \text{otherwise.} \end{cases} \tag{4}$$

Note that the strict monotony guarantees the existence of the inverse. If the function $g_i(x) = C_i$ is constant on $x \in (a, b)$, its CPD is given by

$$\rho_i(x) = \delta(x - C_i), \tag{5}$$

where $\delta(\cdot)$ denotes the Dirac distribution.

Definition 3. Let g be a piecewise, continuously differentiable, periodic function with the time period T defined by

$$g : \begin{cases} (t_{i-1}, t_i) \to \mathbb{R} & \text{for } i = 1, \dots, n, \\ x \mapsto g_i(x), \end{cases} \tag{6}$$

with $t_0 = 0$ and $t_n = T$ such that all g_i are either strictly monotonously increasing, decreasing, or constant on its domain of definition. We further define $\Delta T_i := t_i - t_{i-1}$. Then, the CPD of g is defined by the weighted average

$$\rho(x) := \frac{1}{T} \sum_{i=1}^{n} \Delta T_i \rho_i(x). \tag{7}$$

Theorem 2. *For a bounded function f and an at least piecewise continuously differentiable periodic function g with period T, the averaging operator*

$$\tilde{f}(x_S) = \langle f(x_S + g(t)) \rangle = \frac{1}{T} \int_0^T f(x_S + g(t)) dt \tag{8}$$

15214001, 0, Downloaded from https://onlinelibrary.wiley.com/doi/10.1002/zamm.202300432, Wiley Online Library on [23/03/2024]. See the Terms and Conditions (https://onlinelibrary.wiley.com/terms-and-conditions) on Wiley Online Library for rules of use; OA articles are governed by the applicable Creative Commons License

is equivalent to the cross-correlation integral

$$(\rho \star f)(x_S) = \int_{-\infty}^{\infty} f(x)\rho(x - x_S)dx, \tag{9}$$

if $\rho(x)$ is chosen as the CPD of the "fast" variable $g(t)$.

Proof. Starting at time 0 and ending at T, the time period can be divided into n intervals. In n_I pieces of intervals, the function is strictly monotonously increasing; in n_D, it is strictly monotonously decreasing; and, in $n - n_I - n_D$, it is constant. Let us denote the division points by $t_0 = 0, t_1, \dots t_n = T$. We denote the intervals by

$$T_i = (t_{i-1}, t_i) \subset \mathbb{R} \qquad \text{for } i = 1, \dots, n, \tag{10}$$

and their length by

$$\Delta T_i = t_i - t_{i-1} \in \mathbb{R}^+ \qquad \text{for } i = 1, \dots, n. \tag{11}$$

We define the index sets

$$S_I := \{i \in S_I | g_i \text{ is strictly monotonically increasing on } T_i\}, \tag{12}$$

$$S_D := \{i \in S_D | g_i \text{ is strictly monotonically decreasing on } T_i\}, \tag{13}$$

$$S_C := \{i \in S_C | g_i \text{ is constant on } T_i\}. \tag{14}$$

Applying the three categories, Equation (7) can be written as

$$\rho(x) := \frac{1}{T}\left(\sum_{i\in S_I} \frac{1}{g_i'[g_i^{-1}(x)]}\mathbf{1}_{g_i(T_i)}(x) + \sum_{i\in S_D} \frac{-1}{g_i'[g_i^{-1}(x)]}\mathbf{1}_{g_i(T_i)}(x) + \sum_{i\in S_C} \Delta T_i \delta(x - C_i)\right). \tag{15}$$

Inserting it into Equation (9), we have

$$\begin{aligned}\int_{-\infty}^{\infty} f(x)\rho(x - x_S)\mathrm{d}x = \int_{-\infty}^{\infty} f(x)\frac{1}{T}\Bigg(&\sum_{i\in S_I} \frac{1}{g_i'[g_i^{-1}(x - x_S)]}\mathbf{1}_{g_i(T_i)}(x - x_S) \\ &+ \sum_{i\in S_D} \frac{-1}{g_i'[g_i^{-1}(x - x_S)]}\mathbf{1}_{g_i(T_i)}(x - x_S) + \sum_{i\in S_C} \Delta T_i \delta(x - x_S - C_i)\Bigg)\mathrm{d}x.\end{aligned} \tag{16}$$

Since $f(x)$ is bounded and $\int_{-\infty}^{\infty} |\rho_i(x)|dx = 1$ by definition, the dominated convergence theorem ensures that the integration and summation signs can be interchanged (even if the number of intervals goes to infinity); hence,

$$\begin{aligned}\int_{-\infty}^{\infty} f(x)\rho(x - x_S)\mathrm{d}x = \frac{1}{T}\Bigg(&\sum_{i\in S_I} \int_{-\infty}^{\infty} \frac{f(x)}{g_i'[g_i^{-1}(x - x_S)]}\mathbf{1}_{g_i(T_i)}(x - x_S)\mathrm{d}x - \sum_{i\in S_D} \int_{-\infty}^{\infty} \frac{f(x)}{g_i'[g_i^{-1}(x - x_S)]}\mathbf{1}_{g_i(T_i)}(x - x_S)\mathrm{d}x \\ &+ \sum_{i\in S_C} \Delta T_i \int_{-\infty}^{\infty} f(x)\delta(x - x_S - C_i)\Bigg)\mathrm{d}x\end{aligned} \tag{17}$$

$$= \frac{1}{T}\left(\sum_{i\in S_I} \int_{g_i(t_{i-1})+x_S}^{g_i(t_i)+x_S} \frac{f(x)}{g_i'[g_i^{-1}(x - x_S)]}\mathrm{d}x - \sum_{i\in S_D} \int_{g_i(t_i)+x_S}^{g_i(t_{i-1})+x_S} \frac{f(x)}{g_i'[g_i^{-1}(x - x_S)]}\mathrm{d}x + \sum_{i\in S_C} \Delta T_i f(x_S + C_i)\right), \tag{18}$$

15214001, 0, Downloaded from https://onlinelibrary.wiley.com/doi/10.1002/zamm.202300432, Wiley Online Library on [23/03/2024]. See the Terms and Conditions (https://onlinelibrary.wiley.com/terms-and-conditions) on Wiley Online Library for rules of use; OA articles are governed by the applicable Creative Commons License

where the last summation term is obtained by using the sifting property of the Dirac distribution. Note that in the case of decreasing intervals, the lower boundary of $g(T_i)$ is at $g(t_i)$, and the upper boundary is at $g(t_{i-1})$. Thus, a change in the integration boundaries will cancel out the minus sign as follows:

$$\int_{-\infty}^{\infty} f(x)\rho(x-x_S)\mathrm{d}x = \frac{1}{T}\left(\sum_{i\in S_I}\int_{g_i(t_{i-1})+x_S}^{g_i(t_i)+x_S}\frac{f(x)}{g_i'[g_i^{-1}(x-x_S)]}\mathrm{d}x + \sum_{i\in S_D}\int_{g_i(t_{i-1})+x_S}^{g_i(t_i)+x_S}\frac{f(x)}{g_i'[g_i^{-1}(x-x_S)]}\mathrm{d}x + \sum_{i\in S_C}\Delta T_i f(x_S+C_i)\right). \tag{19}$$

Now, in every non-constant interval of f, we introduce the following variable transformations, respectively,

$$x = x_S + g_i(t), \qquad x_S = x - g_i(t), \qquad \mathrm{d}x = g_i'(t)\mathrm{d}t, \qquad t = g_i^{-1}(x-x_S), \tag{20}$$

and we substitute them into Equation (19)

$$\int_{-\infty}^{\infty} f(x)\rho(x-x_S)\mathrm{d}x = \frac{1}{T}\left(\sum_{i\in S_I}\int_{t_{i-1}}^{t_i}\frac{f(x_S+g_i(t))}{g_i'[g_i^{-1}(g_i(t))]}g_i'(t)\mathrm{d}t + \sum_{i\in S_D}\int_{t_{i-1}}^{t_i}\frac{f(x_S+g_i(t))}{g_i'[g_i^{-1}(g_i(t))]}g_i'(t)\mathrm{d}t + \sum_{i\in S_C}\Delta T_i f(x_S+C_i)\right) \tag{21}$$

$$= \frac{1}{T}\left(\sum_{i\in S_I}\int_{t_{i-1}}^{t_i} f(x_S+g_i(t))\mathrm{d}t + \sum_{i\in S_D}\int_{t_{i-1}}^{t_i} f(x_S+g_i(t))\mathrm{d}t + \sum_{i\in S_C}\int_{t_{i-1}}^{t_i} f(x_S+\underbrace{g_i(t)}_{=C_i})\mathrm{d}t\right) \tag{22}$$

$$= \frac{1}{T}\int_0^T f(x_S+g(t))\mathrm{d}t. \tag{23}$$

□

Remark 1. In technically relevant applications, almost periodic "fast" motions, such as, for example, the sum of two sines with incommensurable frequencies, often arise. Choosing the interval boundaries will influence the result if one wants to average such functions over a finite time interval. $g(t)$ being almost periodic, no time period exists in this case. However, one can take $T \to \infty$ to obtain a uniquely defined integral (cf. Section 3.2.1).

This result is important for several reasons; it facilitates the calculation of averaged values in the case of piecewise-defined functions. Further, the numerical calculation of averaged values also becomes simpler since, numerically, the CPD is very easy to obtain; it is enough to evaluate the "fast" movement on a time period in N pieces of equidistantly positioned time instants and to make the histogram of the obtained data. It is well known that for $N \to \infty$, the histogram approaches the PDF/CPD [36].

Corollary 1. *Since Equation (9) is the cross-correlation of the functions $f(x)$ and $\rho(x)$, the averaging problem in Theorem 2 can be transformed into the Fourier domain if the product $f(x)\rho(x-x_S)$ is $L^1(\mathbb{R})$. (By the boundedness of $f(x)$, this criterion can always be ensured by multiplying $f(x)$ with a window function $w(x)$ to restrict it to the technically relevant region. The area under the curve of $\rho(x)$ is 1 by definition; thus $w(x)f(x)\rho(x-x_S) \in L^1(\mathbb{R})$). The cross-correlation integral in the Fourier domain becomes a product, and through inverse Fourier transformation, the averaged function can be obtained rapidly, that is,*

$$\mathcal{F}\{\rho \star f\} = \overline{\mathcal{F}\{\rho\}} \cdot \mathcal{F}\{f\}. \tag{24}$$

The numerical calculation of the averaged value of $f(x)$ can also be performed using effective methods relying on the numerical equivalents of the Fourier transformation, for example, the fast Fourier transform (FFT) algorithm.

Corollary 2. *Equation (9) remains valid if the "fast" variable x_F depends on x_S, that is, $x_F = g(t, x_S)$.*

Proof. It is easy to see that x_S plays the role of a constant through the calculations; thus, the proof remains valid if we allow the dependency of the "fast" variable on the "slow" one. □

15214001, 0, Downloaded from https://onlinelibrary.wiley.com/doi/10.1002/zamm.202300432, Wiley Online Library on [23/03/2024]. See the Terms and Conditions (https://onlinelibrary.wiley.com/terms-and-conditions) on Wiley Online Library for rules of use; OA articles are governed by the applicable Creative Commons License

Corollary 3. *Assume that* $m_1 = \int_{-\infty}^{\infty} x\rho(x)dx = 0$. *By this and the fact that* $m_0 = \int_{-\infty}^{\infty} \rho(x)dx = 1$, *affine functions, that is, of the form* $f(x) = ax + b$, *remain unchanged under the application of the cross-correlation integral. Therefore, under the above assumptions, affine functions are eigenfunctions of the averaging operator with eigenvalue* $\lambda = 1$.

Proof.

$$\tilde{f}(y) = \int_{-\infty}^{\infty} (ax + b)\rho(x - y)\mathrm{d}x = a \underbrace{\int_{-\infty}^{\infty} x\rho(x - y)\mathrm{d}x}_{=y} + b \underbrace{\int_{-\infty}^{\infty} \rho(x - y)\mathrm{d}x}_{=1} = ay + b. \tag{25}$$

□

Definition 4. The k^{th} *moment* of a random variable X described by its PDF $\rho(x)$ is defined by

$$m_k = \mathrm{E}(X^k) = \int_{-\infty}^{\infty} x^k \rho(x)\mathrm{d}x. \tag{26}$$

Definition 5. The k^{th} *partial moment* of a random variable X described by its PDF $\rho(x)$ is defined by

$$m_k(x) = \mathrm{E}_x(X^k) = \int_{-\infty}^{x} y^k \rho(y)\mathrm{d}y. \tag{27}$$

Lemma 1. *All partial moments of* $\rho(x)$ *are bounded and exist if the range of* $g(t)$ *is bounded.*

Proof. Let $F(x) = \int_{-\infty}^{x} \rho(\tilde{x})\mathrm{d}\tilde{x}$ denote the cumulative density function of X. Since the range of $g(t)$ is bounded, $\rho(x)$ has compact support with $x_l := \inf g(t)$ and $x_u := \sup g(t)$. In the range of interest, we have $x_l < x < x_u$. Since $\rho(x)$ is a PDF, $\int_{-\infty}^{\infty} \rho(x)\mathrm{d}x = 1$. Let us define

$$L_k(x) = \min_{y \in (x_l, x)} y^k \quad \text{and} \quad U_k(x) = \max_{y \in (x_l, x)} y^k. \tag{28}$$

Then, we have

$$L_k(x)F(x) = L_k(x) \int_{x_l}^{x} \rho(y)\mathrm{d}y = \int_{-\infty}^{x} L_k(x)\rho(y)\mathrm{d}y \le \int_{-\infty}^{x} y^k \rho(y)\mathrm{d}y \le \int_{-\infty}^{x} U_k(x)\rho(y)\mathrm{d}y = U_k(x) \int_{x_l}^{x} \rho(y)\mathrm{d}y = U_k(x)F(x). \tag{29}$$

Thus, all partial moments are bounded and therefore exist. By inserting $x = x_u$, it is also shown that all moments exist. □

Theorem 3. *Assume that* $f(x)$ *is a real analytic function and has the domain of convergence* $D(y) = (y + R_l(y), y + R_u(y))$ *when expanded into Taylor series around* y *with the non-positive valued function* $R_l(y)$ *and the non-negative valued one* $R_u(y)$. *Furthermore, assume that the range of the "fast" variable* $g(t)$ *is* $[x_l, x_u]$, *that is,* $\sup g(t) = x_u$ *and* $\inf g(t) = x_l$. *Without loss of generality, we assume* $m_1 = 0$, *and thus* $x_l \le 0 \le x_u$. *We define the set*

$$D_\rho = \{(y \in \mathbb{R} | (R_l(y) < x_l) \wedge (x_u < R_u(y))\}, \tag{30}$$

that is, the set of points around which the convergence radius of $f(x)$ *is large enough that the support of* $\rho(x)$ *fits into it (cf. Figure 1). Then, the following holds.*

$$\tilde{f}(y) = \int_{-\infty}^{\infty} f(x)\rho(x - y)dx = \sum_{k=0}^{\infty} m_k \frac{f^{(k)}(y)}{k!} \quad \text{for } y \in D_\rho, \tag{31}$$

where $(\cdot)^{(k)}(x)$ *denotes the* k^{th} *derivative.*

15214001, 0, Downloaded from https://onlinelibrary.wiley.com/doi/10.1002/zamm.202300432, Wiley Online Library on [23/03/2024]. See the Terms and Conditions (https://onlinelibrary.wiley.com/terms-and-conditions) on Wiley Online Library for rules of use; OA articles are governed by the applicable Creative Commons License

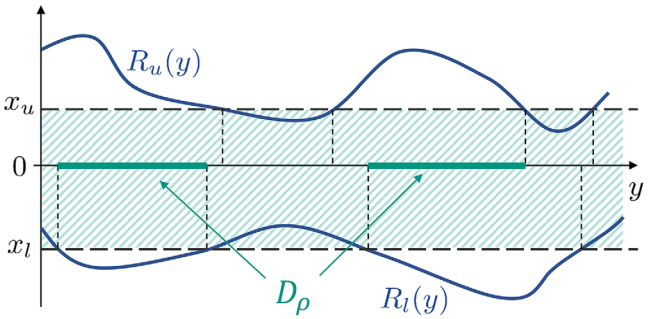

FIGURE 1 Visual interpretation of the definition of D_ρ.

Proof. Taylor expansion of $f(x)$ around y and interchanging the summation and integral signs (allowed due to dominated convergence) yields

$$\tilde{f}(y) = \int_{-\infty}^{\infty} \left(\sum_{k=0}^{\infty} \frac{f^{(k)}(y)}{k!} (x-y)^k \right) \rho(x-y) \mathrm{d}x = \sum_{k=0}^{\infty} \left(\frac{f^{(k)}(y)}{k!} \int_{-\infty}^{\infty} x^k \rho(x) \mathrm{d}x \right) = \sum_{k=0}^{\infty} m_k \frac{f^{(k)}(y)}{k!} \quad \text{for } y \in D_\rho. \tag{32}$$

□

Equation (31) shows that the feasibility of obtaining an analytic expression for the averaged value of $f(x_S + g(t))$ depends solely on whether the corresponding moments of $\rho(x)$ are known. Often, the moments can be obtained with the moment-generating function or the characteristic function of the corresponding CPD/PDF. Furthermore, the moments can be estimated easily if an equidistant experimental/simulation time series of the "fast" motion is available:

$$\hat{m}_k = \frac{\sum_{i=1}^{n} x_i^k}{n}, \tag{33}$$

where x_i is the i^{th} time instance in the n-element data series. The variance of the moments estimator is obtained by

$$\mathrm{Var}(\hat{m}^k) = \mathrm{Var}\left(\frac{\sum_{i=1}^{n} X_i^k}{n} \right) = \frac{\mathrm{Var}(X_1^k)}{n} = \frac{m_{2k} - m_k^2}{n}. \tag{34}$$

Equation (34) shows that the estimator becomes more accurate with a larger sample size. However, higher moments are more sensitive to the tails of the distribution. Therefore, noisy measurement data require a larger sample size to obtain accurate estimates for higher moments.

Theorem 3 is especially important in two cases: (a) the target function is a polynomial; thus, only a finite number of moments are needed to obtain the average, or (b) the support of ρ is small, and for $k \to \infty$, we have $m^k \to 0$. We prove this second statement in the following.

Corollary 4. *We keep the assumptions of Theorem 3 and further assume that ρ has short support, that is, $x_u - x_l = \varepsilon$. We also assume that all derivatives of the target function $f^{(k)}(y)$ are of magnitude $\mathcal{O}(1)$. Then, the difference between the original and the averaged target function $\tilde{f}(y) - f(y)$ is uniformly of $\mathcal{O}(\varepsilon^2)$ for $y \in D_\rho$.*

Proof. By the fact that ρ is a PDF and by the assumption $m_1 = 0$, Theorem 3 yields

$$\tilde{f}(y) = f(y) + \sum_{k=2}^{\infty} m_k \frac{f^{(k)}(y)}{k!} \quad \text{for } y \in D_\rho. \tag{35}$$

We also have $-\varepsilon \le x_l \le 0 \le x_u \le \varepsilon$ and make use of Lemma 1 by setting $L_k(x) = -|x_l|^k$ and $U_k(x) = x_u^k$, thus the moments are bounded by

$$-\varepsilon^k \le m_k \le \varepsilon^k, \tag{36}$$

15214001, 0, Downloaded from https://onlinelibrary.wiley.com/doi/10.1002/zamm.202300432, Wiley Online Library on [23/03/2024]. See the Terms and Conditions (https://onlinelibrary.wiley.com/terms-and-conditions) on Wiley Online Library for rules of use; OA articles are governed by the applicable Creative Commons License

hence

$$\tilde{f}(y) = f(y) + \mathcal{O}(\varepsilon^2), \tag{37}$$

and

$$|\tilde{f}(y) - f(y)| = \mathcal{O}(\varepsilon^2) \quad \text{for } y \in D_\rho. \tag{38}$$

□

It is an important implication since it shows that under the above assumptions, sufficiently smooth functions are not altered much by averaging if the "fast" variable has a small range. Furthermore, since $\varepsilon < 1$ we also have $\lim_{k\to\infty} \varepsilon^k = 0$.

The averaging method might also be applied when defining the target function piecewise. Similar results can be formulated using partial moments of the "fast" motion's CPD.

Theorem 4. *Assume that the range of the "fast" variable $g(t)$ is $[x_l, x_u]$, that is, $x_u = \sup g(t)$ and $x_l = \inf g(t)$. Without loss of generality, we assume $m_1 = 0$, thus $x_l \le 0 \le x_u$. Let the target function $f(x)$ be composed of m pieces of analytic functions $f_i(x)$ with $i \in \mathcal{I} := \{1, \dots, m\}$, that is,*

$$f(x) = \sum_{i=1}^{m} f_i(x)\mathbf{1}_{(x_{i-1},x_i)}(x), \tag{39}$$

with $f_i(x)$ convergent on the domains $D_i(y) = (y + R_{l,i}(y), y + R_{u,i}(y))$ when expanded into Taylor series around y, where $R_{l,i}(y)$ and $R_{u,i}(y)$ are nonpositive and nonnegative functions, respectively. Let the domain boundaries be given by $x_0, \dots, x_m$ with $x_0 = -\infty$ and $x_m = \infty$. We denote the domains by $d_i := [x_{i-1}, x_i]$. Furthermore, we define the set-valued function

$$\mathcal{I}_A(y) := \{i \in \mathcal{I} | d_i \cap [y + x_l, y + x_u] \neq \emptyset\} \tag{40}$$

denoting the indices of the set of active functions, that is, those where $\rho(x - y) > 0$ for any $x \in [x_{i-1}, x_i]$. We define

$$D(y) := \bigcap_{i\in\mathcal{I}_A(y)} D_i(y) \quad \Longrightarrow \quad D(y) = (y + R_l(y), y + R_u(y)) \tag{41}$$

with

$$R_l(y) := \max_{i\in\mathcal{I}_A(y)} R_{l,i}(y) \quad \text{and} \quad R_u(y) := \min_{i\in\mathcal{I}_A(y)} R_{u,i}(y). \tag{42}$$

Furthermore, we define D_ρ as in Theorem 3. Then,

$$\tilde{f}(y) = \sum_{i\in\mathcal{I}_A(y)} \sum_{k=0}^{\infty} \frac{f_i^{(k)}(y)}{k!}(m_k(x_i - y) - m_k(x_{i-1} - y)) \quad \text{for } y \in D_\rho, \tag{43}$$

where $m_k(x)$ denotes the k^{th} partial moment as defined in Definition 5.

Proof. As long as $x \in D(y)$, we can evaluate $f(x)$ using its Taylor expansion around any y by

$$f(x) = \sum_{i\in\mathcal{I}_A(y)} f_i(x)\mathbf{1}_{(x_{i-1},x_i)}(x) = \sum_{i\in\mathcal{I}_A(y)} \left(\sum_{k=0}^{\infty} \frac{f_i^{(k)}(y)}{k!}(x - y)^k \right) \mathbf{1}_{(x_{i-1},x_i)}(x), \quad \text{for } x \in D(y). \tag{44}$$

Inserting Equation (44) in the integral Equation (9), we have

$$\tilde{f}(y) = \int_{-\infty}^{\infty} f(x)\rho(x - y)\mathrm{d}x = \int_{-\infty}^{\infty} \left(\sum_{i\in\mathcal{I}_A(y)} \left(\sum_{k=0}^{\infty} \frac{f_i^{(k)}(y)}{k!}(x - y)^k \right) \mathbf{1}_{(x_{i-1},x_i)}(x) \right) \rho(x - y)\mathrm{d}x \tag{45}$$

$$= \int_{-\infty}^{\infty} \sum_{i\in\mathcal{I}_A(y)} \left(\sum_{k=0}^{\infty} \frac{f_i^{(k)}(y)}{k!} x^k \rho(x) \right) \mathbf{1}_{(x_{i-1}-y,x_i-y)}(x)\mathrm{d}x, \tag{46}$$

15214001, 0, Downloaded from https://onlinelibrary.wiley.com/doi/10.1002/zamm.202300432, Wiley Online Library on [23/03/2024]. See the Terms and Conditions (https://onlinelibrary.wiley.com/terms-and-conditions) on Wiley Online Library for rules of use; OA articles are governed by the applicable Creative Commons License

and by dominated convergence, summation and integral signs can be interchanged, leading to

$$\tilde{f}(y) = \sum_{i\in\mathcal{I}_A(y)} \sum_{k=0}^{\infty} \frac{f_i^{(k)}(y)}{k!} \left(\int_{-\infty}^{\infty} x^k \rho(x) \mathbf{1}_{(x_{i-1}-y, x_i-y)}(x) \mathrm{d}x \right) \tag{47}$$

$$= \sum_{i\in\mathcal{I}_A(y)} \sum_{k=0}^{\infty} \frac{f_i^{(k)}(y)}{k!} \left(\int_{x_{i-1}-y}^{x_i-y} x^k \rho(x) \mathrm{d}x \right) \tag{48}$$

$$= \sum_{i\in\mathcal{I}_A(y)} \sum_{k=0}^{\infty} \frac{f_i^{(k)}(y)}{k!} (m_k(x_i - y) - m_k(x_{i-1} - y)) \quad \text{for } y \in D_\rho. \tag{49}$$

□

Equation (43) shows that knowledge of the partial moments of the "fast" variable's CPD is sufficient to calculate the average of the target function.

The following two examples demonstrate the usefulness of Theorems 3 and 4.

Example 1. We calculate the average of $f(x + g(t))$ with $f(x) = x^2$ and $g(t) = A\sin(\omega t)$. The average can be obtained classically by calculating

$$\tilde{f}(x) = \frac{\omega}{2\pi} \int_0^{2\pi/\omega} (x + A\sin\omega t)^2 \mathrm{d}t = \frac{\omega}{2\pi} \int_0^{2\pi/\omega} \left(x^2 + 2xA\sin\omega t + A^2\sin^2\omega t \right) \mathrm{d}t = x^2 + \frac{A^2}{2}. \tag{50}$$

Alternatively, the averaged function can be calculated using Equation (31). It is well known that the CPD of a harmonic motion (cf. Equation 84) with amplitude A is given by the arcsine distribution [36] with half-width A. The derivation of its moments is given in Appendix A. For now, the moments are relevant up to the second order: $m_0 = 1$, $m_1 = 0$, and $m_2 = A^2/2$. Furthermore, $f'(x) = 2x$ and $f''(x) = 2$ and $f^{(k)}(x) = 0$ for $k > 2$. Thus, by Equation (31),

$$\tilde{f}(x) = m_0 f(x) + m_1 f'(x) + m_2 \frac{f''(x)}{2} = x^2 + \frac{A^2}{2}. \tag{51}$$

Example 2. Calculate the average of $f(x + g(t))$ with

$$f(x) = \begin{cases} x & \text{for } |x| < 1 \\ 0 & \text{otherwise.} \end{cases} \quad \text{and} \quad g(t) = A\sin(\omega t) \quad \text{with } A < 1. \tag{52}$$

Using Theorem 4, we have $m = 3$,

$$x_0 = -\infty, \qquad x_1 = -1, \qquad x_2 = 1, \qquad x_3 = \infty, \tag{53}$$

and

$$f_1(y) = 0, \qquad f_2(y) = y, \qquad f_2'(y) = 1, \qquad f_3(y) = 0 \qquad \text{with} \quad D(y) = \mathbb{R} \quad \text{for } y \in \mathbb{R}, \tag{54}$$

hence, $D_\rho = \mathbb{R}$. The active set is

$$\mathcal{I}_A(y) = \begin{cases} \{1\} & \text{for } y < -1 - A, \\ \{1, 2\} & \text{for } -1 - A < y < -1 + A, \\ \{2\} & \text{for } -1 + A < y < 1 - A, \\ \{2, 3\} & \text{for } 1 - A < y < 1 + A, \\ \{3\} & \text{for } 1 + A < y, \end{cases} \tag{55}$$

15214001, 0, Downloaded from https://onlinelibrary.wiley.com/doi/10.1002/zamm.202300432, Wiley Online Library on [23/03/2024]. See the Terms and Conditions (https://onlinelibrary.wiley.com/terms-and-conditions) on Wiley Online Library for rules of use; OA articles are governed by the applicable Creative Commons License

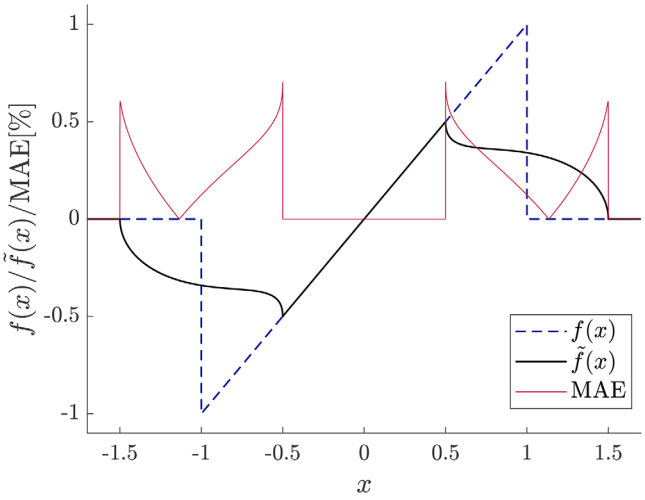

FIGURE 2 Absolute error [%] of the numerical cross correlation with $N_x = 2^{13} + 1$ grid points on $(-1.7, 1.7)$. $f(x) = x \cdot \mathbf{1}_{(-1,1)}(x)$ and $g(t) = 0.5 \sin t$. The analytic expression of the averaged function $\tilde{f}(x)$ is given in Equation (57).

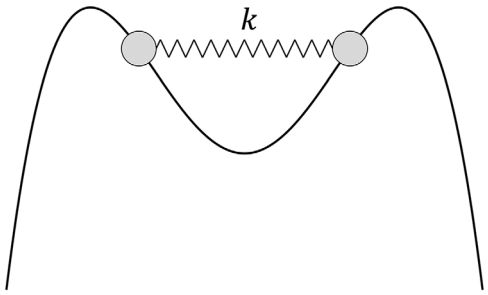

FIGURE 3 Problem setting—a pair of coupled particles in a quadratic-quartic potential well.

and by Equation (43),

$$\tilde{f}(y) = y(m_0(1-y) - m_0(-1-y)) + m_1(1-y) - m_1(-1-y), \tag{56}$$

and using Equation (A13), we find

$$\tilde{f}(y) = \begin{cases} 0 & \text{for } y \le -1 - A, \\ y/2 + \pi^{-1}\left[\sqrt{A^2 - (1+y)^2} + y \arcsin\left((1+y)/A\right)\right] & \text{for } -1 - A < y \le -1 + A, \\ y & \text{for } -1 + A < y \le 1 - A, \\ y/2 - \pi^{-1}\left[\sqrt{A^2 - (1-y)^2} - y \arcsin\left((1-y)/A\right)\right] & \text{for } 1 - A < y \le 1 + A, \\ 0 & \text{for } 1 + A < y. \end{cases} \tag{57}$$

For a graphical representation with $A = 0.5$, see Figure 2.

Example 3. We are interested in the escape of two particles coupled by a strong linear spring of stiffness $k \gg 1$ in a quadratic–quartic potential well $V(x) = x^2/2 - x^4/4$ (cf. Figure 3). The equations of motion are given by

$$\ddot{x}_1 + V'(x_1) + k(x_1 - x_2) = 0, \tag{58}$$

$$\ddot{x}_2 + V'(x_2) + k(x_2 - x_1) = 0, \tag{59}$$

$$x_1(0) = x_2(0) = 0, \tag{60}$$

$$\dot{x}_1(0) = -v_0, \tag{61}$$

$$\dot{x}_2(0) = v_0. \tag{62}$$

15214001, 0, Downloaded from https://onlinelibrary.wiley.com/doi/10.1002/zamm.202300432, Wiley Online Library on [23/03/2024]. See the Terms and Conditions (https://onlinelibrary.wiley.com/terms-and-conditions) on Wiley Online Library for rules of use; OA articles are governed by the applicable Creative Commons License

Introducing the new variables center of mass and relative displacement

$$y_1 = \frac{x_1 + x_2}{2}, \qquad \text{and} \qquad y_2 = x_2 - x_1, \tag{63}$$

we obtain

$$\ddot{y}_1 + \frac{V'\left(y_1 - \frac{y_2}{2}\right) + V'\left(y_1 + \frac{y_2}{2}\right)}{2} = 0, \tag{64}$$

$$\ddot{y}_2 + \left(2k + 1 - 3y_1^2\right) y_2 - \frac{y_2^3}{4} = 0, \tag{65}$$

$$y_1(0) = \dot{y}_1(0) = 0, \tag{66}$$

$$y_2(0) = 0, \tag{67}$$

$$\dot{y}_2(0) = 2v_0. \tag{68}$$

Since $V'(x)$ is even, $y_1(t) = 0$ is a solution; however, its stability needs to be clarified and will depend on the values of v_0 and k. By inserting $y_1(t)$ in Equation (65), the problem is reduced to an SDO with parameters $c_1 = 2k + 1$ and $c_3 = -1/4$ (cf. Section 3.1.3). The total energy is given by

$$E_0 = \frac{1}{2}\dot{y}_2^2(0) = 2v_0^2, \tag{69}$$

which determines the amplitude of the vibrations

$$A = 2\sqrt{2k+1}\sqrt{1 - \sqrt{1 - \frac{2v_0^2}{(2k+1)^2}}}. \tag{70}$$

Since $k \gg 1$, the vibrations in y_2 are "fast", and we can average Equation (64). By Theorem 2, it is not necessary to exactly determine $y_2(t)$; its CPD suffices. Theorem 3 shows that only the first three moments will play a role in the averaging since $V'(x)$ is a polynomial of degree three. Since $y_2(t)$ is symmetric, the odd moments are zero and the only moment left (besides the trivial zeroth one) is the second one, given by Equation (C10). Since $c_1 \gg |c_3|$, the motion does not differ much from a harmonic motion having the second moment given by Equation (85)

$$m_{y_2,2} = \frac{A^2}{2}. \tag{71}$$

We introduce the averaged center of mass $\xi := \langle y_1 \rangle$. After rescaling the moment due to the factor $1/2$, insertion into Equation (71) yields

$$\left\langle V'\left(y_1 - \frac{y_2(t)}{2}\right)\right\rangle = \left\langle V'\left(y_1 + \frac{y_2(t)}{2}\right)\right\rangle = V'(\xi) + \frac{1}{8}V'''(\xi)m_{y_2,2} = \left(1 - \frac{3}{8}A^2\right)\xi - \xi^3, \tag{72}$$

resulting in the averaged differential equation

$$\ddot{\xi} + \left(1 - \tfrac{3}{8}A^2\right)\xi - \xi^3 = 0. \tag{73}$$

Linear stability analysis yields the stability condition

$$\frac{8}{3} \overset{!}{>} A^2, \tag{74}$$

which is equivalent to

$$v_0 \overset{!}{<} v_{0,c} := \frac{2}{3}\sqrt{3k+1}. \tag{75}$$

15214001, 0, Downloaded from https://onlinelibrary.wiley.com/doi/10.1002/zamm.202300432, Wiley Online Library on [23/03/2024]. See the Terms and Conditions (https://onlinelibrary.wiley.com/terms-and-conditions) on Wiley Online Library for rules of use; OA articles are governed by the applicable Creative Commons License

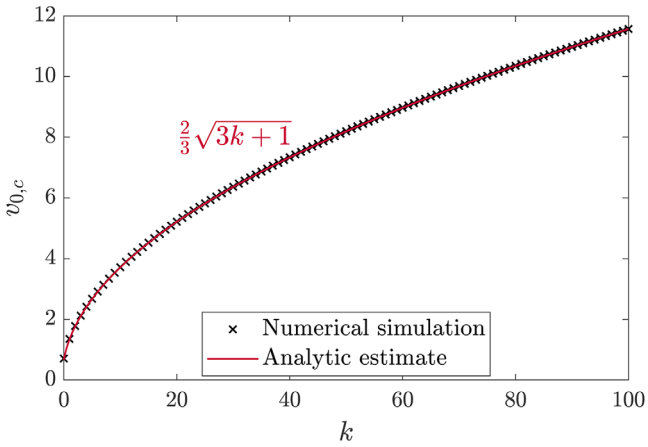

FIGURE 4 The critical value of the initial velocity $v_{0,c}$ depicted against the stiffness of the linear spring k.

A comparison of the analytic estimate with direct numerical simulations is shown in Figure 4. The numerical simulations were obtained by disturbing the initial conditions by setting $y_1(0) = 0.005$ and integrating the system up to 1000 time units. If the particle pair escapes, the solution $y_1(t) = 0$ is classified as unstable.

3 | OBTAINING THE CLASSICAL PROBABILITY DENSITY

An analytic expression of the CPD of the motion $x_F(t) \equiv g(t)$ is rarely available. However, in some simple cases, it can be derived [32, 34]. In this section, we recapitulate some of the most important CPDs that rely on a particle's undamped motion in a potential and provide a novel example for calculating a more complex motion consisting of the sum of two incommensurable harmonics.

3.1 | CPD of undamped, free oscillations

The PDF/CPD of a function in the form as given in Equation (3) originates from probability theory and is not related to particle motion [35]. However, an equivalent physical definition can also be given [32]. Consider that the particle performs a unidirectional motion $x(t)$ from $x(a) = x_a$ to $x(b) = x_b$ with $a < b$. The particle spends $\mathrm{d}t$ amount of time in an infinitesimally small region of this interval $\mathrm{d}x$, where

$$\mathrm{d}t = \frac{\mathrm{d}x}{\mathrm{d}x/\mathrm{d}t} = \frac{\mathrm{d}x}{v(x)}, \tag{76}$$

being inversely proportional to the particle's velocity. The probability $\rho(x)$ of finding the particle in this infinitesimal region is the ratio of the time spent here to the total amount of time $b - a$ needed from x_a to x_b, that is,

$$\rho(x)\mathrm{d}x \equiv \text{Probability}[(x, x + \mathrm{d}x)] = \frac{\mathrm{d}t}{b-a} = \frac{1}{b-a}\frac{\mathrm{d}x}{v(x)}, \tag{77}$$

hence,

$$\rho(x) = \frac{1}{b-a}\frac{1}{v(x)}. \tag{78}$$

Often the time and not the displacement dependency of the velocity is known, that is, $v(t) = \mathrm{d}x/\mathrm{d}t \equiv g'(t)$, so we have to express t in terms of x and rewrite Equation (78) as

$$\rho(x) = \frac{1}{b-a}\frac{1}{g'(g^{-1}(x))} \quad \text{for } x \in (x_a, x_b). \tag{79}$$

15214001, 0, Downloaded from https://onlinelibrary.wiley.com/doi/10.1002/zamm.202300432, Wiley Online Library on [23/03/2024]. See the Terms and Conditions (https://onlinelibrary.wiley.com/terms-and-conditions) on Wiley Online Library for rules of use; OA articles are governed by the applicable Creative Commons License

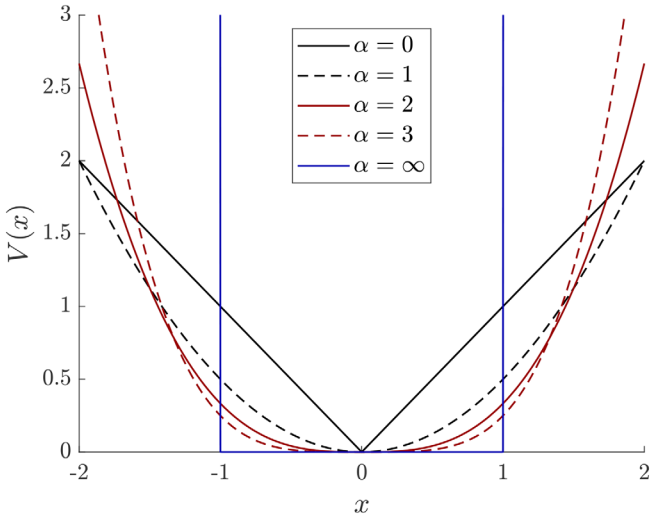

(a) Potentials of PNOs $V(x) = |x|^{\alpha+1}/(\alpha+1)$ for different values of the parameter α

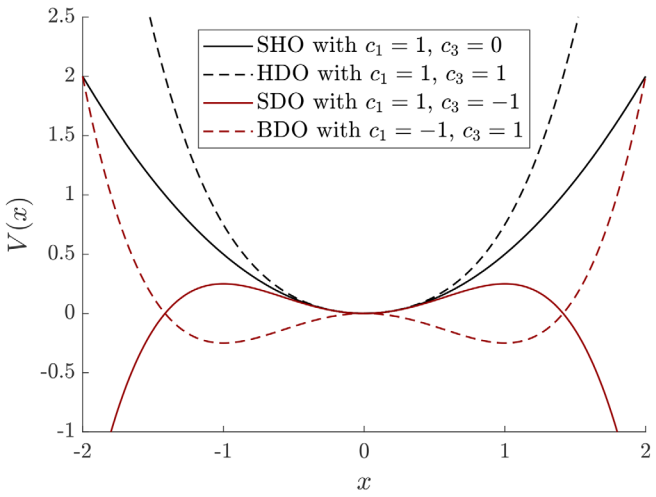

(b) Potentials of DTOs $V(x) = c_1 \frac{x^2}{2} + c_3 \frac{x^4}{4}$ for different values of the parameters c_1 and c_3

FIGURE 5 Common potentials. The corresponding probability density functions are calculated in the next sections.

Equation (79) is useful when the velocity is known as a function of the time, whereas Equation (78) is preferred when the velocity is known as a function of the displacement. The latter is the case when an undamped particle of unit mass oscillates freely in a potential well between the turning points x_a and x_b with the time period τ. Based on the conservation of energy, we have

$$E = T + V = \frac{1}{2}v^2 + V(x), \tag{80}$$

thus insertion of

$$v(x) = \sqrt{2(E - V(x))} \tag{81}$$

into Equation (78) yields

$$\rho(x) = \frac{2}{\tau}\sqrt{\frac{1}{2(E - V(x))}}. \tag{82}$$

The factor $2/\tau$, including the time period of the oscillation, normalizes the area of $\rho(x)$ to one. τ is given by the integral [1]

$$\tau = 2\int_{x_a}^{x_b} \frac{1}{\sqrt{2(E - V(x))}} \mathrm{d}x. \tag{83}$$

In the following, we give some examples of potentials usually found in applications. Figure 5 shows examples of the so-called purely nonlinear oscillators (PNOs) and Duffing-type oscillators (DTOs).

3.1.1 | CPD and moments of a simple harmonic oscillation

Arguably, the most important analytically solvable case is that of a harmonic response of amplitude A. As described by Robinett [32], the CPD is given as

$$\rho_{\mathrm{SHO}}(x) = \frac{1}{\pi}\frac{1}{\sqrt{A^2 - x^2}}\mathbf{1}_{(-A,A)}(x). \tag{84}$$

15214001, 0, Downloaded from https://onlinelibrary.wiley.com/doi/10.1002/zamm.202300432, Wiley Online Library on [23/03/2024]. See the Terms and Conditions (https://onlinelibrary.wiley.com/terms-and-conditions) on Wiley Online Library for rules of use; OA articles are governed by the applicable Creative Commons License

The moments are given by

$$m_k = \begin{cases} A^k \frac{1}{2^k} \binom{k}{k/2} & \text{for } k \text{ even}, \\ 0 & \text{for } k \text{ odd}, \end{cases} \quad \text{for } k \geq 1. \tag{85}$$

For further details on the moments of ρ_{SHO}, please refer to Appendix A.

3.1.2 | The CPD of the purely nonlinear oscillator

PNOs have a potential that, after nondimensionalization, can be written as

$$V(x) = \frac{1}{\alpha+1}|x|^{\alpha+1}, \tag{86}$$

where α is a positive real number. The particle has its turning points x_a and x_b at $\pm A$ that depend on the initial energy of the particle E_0:

$$A = (E_0(\alpha+1))^{1/(\alpha+1)}. \tag{87}$$

To determine the CPD, the only challenging task is to calculate the time period's value; the rest is readily given by Equation (82). Fortunately, the problem has been solved by many authors in the past [37–40], and the time period of PNOs is known to be

$$\tau = \underbrace{\sqrt{\frac{8\pi}{\alpha+1}} \frac{\Gamma\left(\frac{1}{\alpha+1}\right)}{\Gamma\left(\frac{1}{2}+\frac{1}{\alpha+1}\right)}}_{T^*(\alpha):=} A^{(1-\alpha)/2} = T^*(\alpha) A^{(1-\alpha)/2}, \tag{88}$$

where Γ denotes the gamma function. $T^*(\alpha)$, a factor only depending on α, is shown in Figure 6a. Thus, the CPD is given by

$$\rho_{\mathrm{PNO}}(x) = \frac{2}{T^*(\alpha)A^{(1-\alpha)/2}} \frac{1}{\sqrt{\frac{2}{\alpha+1}(A^{\alpha+1}-x^{\alpha+1})}} \mathbf{1}_{|x|<A}(x) = \frac{\alpha+1}{2\sqrt{\pi}} \frac{\Gamma\left(\frac{1}{2}+\frac{1}{\alpha+1}\right)}{\Gamma\left(\frac{1}{\alpha+1}\right)} \frac{A^{(\alpha-1)/2}}{\sqrt{A^{\alpha+1}-|x|^{\alpha+1}}} \mathbf{1}_{|x|<A}(x). \tag{89}$$

Important values of α include 1 and the limiting cases $\alpha \to 0^+$ and $\alpha \to \infty$, which correspond to the cases of a simple (linear) harmonic oscillator (SHO), a constant restoring force oscillator, and the so-called "infinite well" [32] oscillator, respectively. Further interesting cases are $\alpha = 2, 3, \ldots$, which might arise if the linear restoring term vanishes during the linearization of a system around an equilibrium position. However, the remaining force can be approximated well by only using one further purely nonlinear term. For a graphical representation of $\rho_{\mathrm{PNO}}(x)$ with different values of α, please refer to Figure 6b. For further details on the moments of ρ_{PNO}, please refer to Appendix B.

3.1.3 | The CPD of Duffing-type oscillators

Undamped DTOs [40] are given in the form

$$\ddot{x} + c_1 x + c_3 x^3 = 0, \tag{90}$$

with real coefficients c_1 and c_3. Based on the signs of these coefficients, there are three cases of interest:

- hardening Duffing oscillator (HDO) for $c_1 > 0$ and $c_3 > 0$,
- softening Duffing oscillator (SDO) for $c_1 > 0$ and $c_3 < 0$,
- bistable Duffing oscillator (BDO) for $c_1 < 0$ and $c_3 > 0$.

15214001, 0, Downloaded from https://onlinelibrary.wiley.com/doi/10.1002/zamm.202300432, Wiley Online Library on [23/03/2024]. See the Terms and Conditions (https://onlinelibrary.wiley.com/terms-and-conditions) on Wiley Online Library for rules of use; OA articles are governed by the applicable Creative Commons License

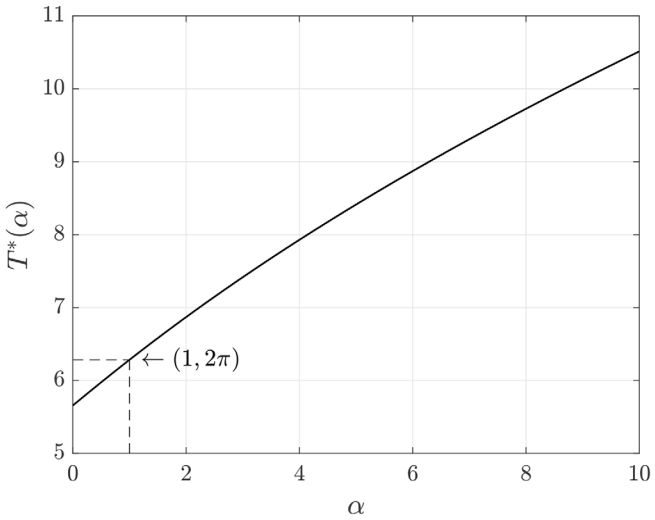

(a) Amplitude independent factor of a PNO's time period $T^*(\alpha)$[40]

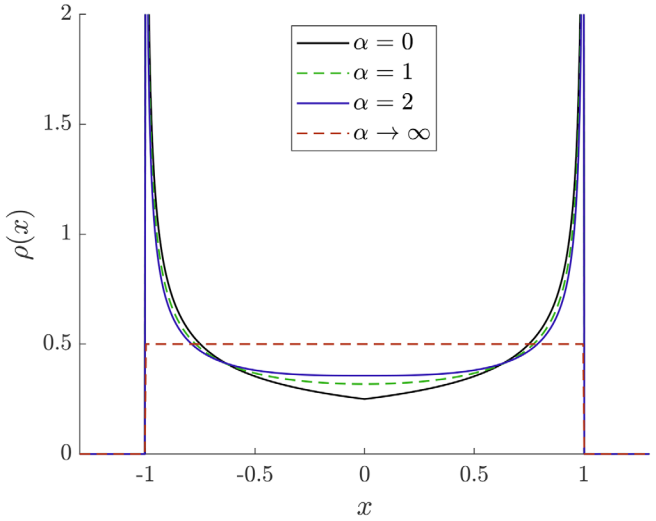

(b) CPD of PNOs with different values of α with initial displacement $A = 1$

FIGURE 6 Purely nonlinear oscillators.

Based on Ref. [40], the time period of the HDO is given by

$$\tau_{\text{HDO}} = \frac{4K\left(\frac{c_3A^2}{2(c_1+c_3A^2)}\right)}{\sqrt{c_1 + c_3A^2}}, \tag{91}$$

where K denotes the complete elliptic integral of the first kind with the elliptic parameter m. Using Equations (82) and (91), the CPD of the HDO is obtained as

$$\rho_{\text{HDO}}(x) = \frac{\sqrt{c_1 + c_3A^2}}{2K\left(\frac{c_3A^2}{2(c_1+c_3A^2)}\right)} \frac{1}{\sqrt{c_1A^2 + \frac{c_3}{2}A^4 - c_1x^2 - \frac{c_3}{2}x^4}}, \tag{92}$$

where $\pm A$ are the turning points of the oscillating particle.

Similarly, for $|A| < \sqrt{c_1/|c_3|}$, the time period of the SDO can be given by

$$\tau_{\text{SDO}} = \frac{4K\left(\frac{c_3A^2}{2(c_1-|c_3|A^2)}\right)}{\sqrt{c_1 - |c_3|A^2}}, \tag{93}$$

hence, the CPD is

$$\rho_{\text{SDO}}(x) = \frac{\sqrt{c_1 - |c_3|A^2}}{2K\left(\frac{c_3A^2}{2(c_1-|c_3|A^2)}\right)} \frac{1}{\sqrt{c_1A^2 - \frac{|c_3|}{2}A^4 - c_1x^2 + \frac{|c_3|}{2}x^4}}. \tag{94}$$

The BDO has two subcases, depending on the particle's energy and thus on its turning points x_a and x_b. For

$$x_a < -\sqrt{\frac{2|c_1|}{c_3}} < \sqrt{\frac{2|c_1|}{c_3}} < x_b, \tag{95}$$

15214001, 0, Downloaded from https://onlinelibrary.wiley.com/doi/10.1002/zamm.202300432, Wiley Online Library on [23/03/2024]. See the Terms and Conditions (https://onlinelibrary.wiley.com/terms-and-conditions) on Wiley Online Library for rules of use; OA articles are governed by the applicable Creative Commons License

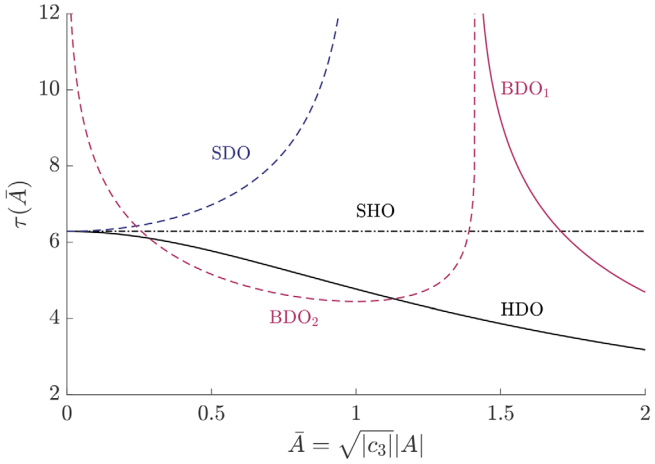

(a) Time periods of different types of non-dimensionalized ($|c_1| = 1$) undamped DTOs depicted against the parameter $\bar{A} = \sqrt{|c_3|}|A|$ [40]

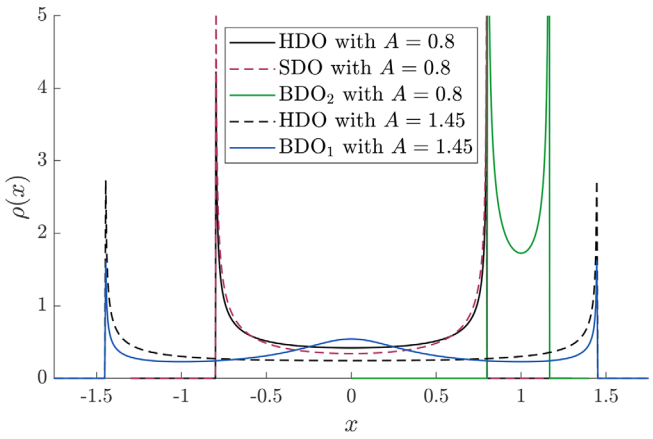

(b) CPDs of the three different types of DTOs with different initial displacement $A = 0.8$ and $A = 1.45$ for $|c_1| = |c_3| = 1$

FIGURE 7 Duffing-type oscillators.

the particle passes through both potential wells, called "full-swing" or "out-of-well mode." We denote this case by BDO$_1$. However, for

$$-\sqrt{\frac{2|c_1|}{c_3}} < x_a < x_b < 0 \qquad \text{or} \qquad 0 < x_a < x_b < \sqrt{\frac{2|c_1|}{c_3}}, \tag{96}$$

the particle oscillates only in one of the potential wells, which is also called the "half-swing" or "in-well mode," and we denote it by BDO$_2$ [40]. When started with zero velocity and initial displacement $x_0 = A$, the particle has the time periods

$$\tau_{\text{BDO}_1} = \frac{4K\left(\frac{c_3A^2}{2(c_3A^2-|c_1|)}\right)}{\sqrt{c_3A^2-|c_1|}}, \qquad \tau_{\text{BDO}_2} = \frac{2K\left(\frac{2(c_3A^2-|c_1|)}{c_3A^2}\right)}{\sqrt{\frac{c_3}{2}}A}, \tag{97}$$

respectively. Then, the CPDs become

$$\rho_{\text{BDO}_1}(x) = \frac{\sqrt{c_3A^2-|c_1|}}{2K\left(\frac{c_3A^2}{2(c_3A^2-|c_1|)}\right)} \frac{1}{\sqrt{c_1A^2+\frac{c_3}{2}A^4-c_1x^2-\frac{c_3}{2}x^4}}, \tag{98}$$

$$\rho_{\text{BDO}_2}(x) = \frac{\sqrt{2c_3}A}{K\left(\frac{2(c_3A^2-|c_1|)}{c_3A^2}\right)} \frac{1}{\sqrt{c_1A^2+\frac{c_3}{2}A^4-c_1x^2-\frac{c_3}{2}x^4}}, \tag{99}$$

respectively. In all four cases, the time periods are functions of c_1 and c_3A^2. Through nondimensionalization, $|c_1| = 1$ can be achieved; thus, the time period becomes a univariate function. Its values are depicted in Figure 7a. Please refer to Figure 7b for a graphical representation of the CPDs of DTOs. For further details on the moments of DTOs, please refer to Appendix C.

3.2 | CPD of forced oscillations

When excitation is present, the energy conservation principle can no longer be applied in the simple form as before, and the use of Equation (78) becomes less viable. Instead, using Equation (79) is more appropriate. However, this approach

15214001, 0, Downloaded from https://onlinelibrary.wiley.com/doi/10.1002/zamm.202300432, Wiley Online Library on [23/03/2024]. See the Terms and Conditions (https://onlinelibrary.wiley.com/terms-and-conditions) on Wiley Online Library for rules of use; OA articles are governed by the applicable Creative Commons License

has a drawback. It requires knowledge of the analytic solution of the forced oscillation, which is typically only available for a few but important cases.

A specific case of nonlinear systems is called *partially strongly damped systems* [24]. These systems consist of "slow" master variables and strongly damped "slaves." In the standard form, such systems can be represented as

$$\dot{x} = \varepsilon X(x, y, t) \tag{100}$$

$$\dot{y} = K(x)y + \varepsilon Y(x, y, t) \tag{101}$$

$$x(0) = x_0, \quad y(0) = y_0, \tag{102}$$

with the assumption

$$\max\left\{eigenvalue\left[\frac{1}{2}(K + K^{\top})\right]\right\} = -1. \tag{103}$$

One can introduce the "slow" variables ξ and η and perform averaging that yields

$$\dot{\xi}_0 = \varepsilon\langle X(\xi_0, \eta_0, t)\rangle_t \tag{104}$$

$$\eta_0 = \exp(K(\xi_0)t)y_0, \quad \xi_0(0) = x_0, \tag{105}$$

$$||x - \xi_0|| = O(\varepsilon), 0 \le t \le O(\varepsilon^{-1}). \tag{106}$$

One implication is that their forced response determines the time evolution of the strongly damped variables. Often, the equations are such that the variable of interest can be described by the sum of a "slow" variable $x_S \equiv \xi_0$ and a "fast" one $x_F \equiv \eta_0$. In the following, we focus on this case assuming only one variable of the form $x = x_S + g(t)$; therefore, Theorem 2 is applicable. We present two typical "fast" motions often encountered in practical applications.

The simplest case is a simple harmonic oscillation, which has already been described in Section 3.1.1. Thus, we will focus on another important case: a biharmonic oscillation.

3.2.1 | The CPD of a biharmonic function with incommensurable frequencies

Let us consider now the CPD of a particle performing the following motion

$$g(t) = \underbrace{A_1 \sin(\omega_1 t + \beta_1)}_{=:g_1(t)} + \underbrace{A_2 \sin(\omega_2 t + \beta_2)}_{=:g_2(t)}, \tag{107}$$

where $A_1, A_2 > 0$ and $\omega_1/\omega_2 \notin \mathbb{R}\backslash\mathbb{Q}$, that is, ω_1 and ω_2 are incommensurable. This motion is obtained as the solution of a harmonically excited undamped harmonic oscillator, where ω_1 is the eigenfrequency of the oscillator and $\omega_2 (\neq \omega_1)$ is the excitation frequency. The same expression emerges as the particular solution of a damped harmonic oscillator under biharmonic excitation (BHO).

To obtain the CPD of $g(t)$, the analytic formula (79) cannot be used anymore since the inverse of the function cannot be given by a closed formula. In addition, the motion is not periodic, implying the assembly of infinitely many terms in Equation (7). If one wants to sample $g(t)$ starting at $t = a$ and ending at $t = b$, the resulting CPD would depend on the values of a and b. However, if the length of the function sample $b - a$ goes to ∞, then Equation (7) converges to a particular limiting function $\rho_{\mathrm{BHO}}(x)$, which can be obtained by convolution of the CPDs/PDFs $\rho_1(x)$ and $\rho_2(x)$. This statement is true because $g(t)$ has the same PDF as the random variable $X := X_1 + X_2$, where X_1 and X_2 are independent random variables following the arcsine distribution centered at 0 with half-width A_1 and A_2. Based on Ref. [41], the PDF of a random variable consisting of the sum of two independent random variables can be calculated by convoluting the PDFs

15214001, 0, Downloaded from https://onlinelibrary.wiley.com/doi/10.1002/zamm.202300432, Wiley Online Library on [23/03/2024]. See the Terms and Conditions (https://onlinelibrary.wiley.com/terms-and-conditions) on Wiley Online Library for rules of use; OA articles are governed by the applicable Creative Commons License

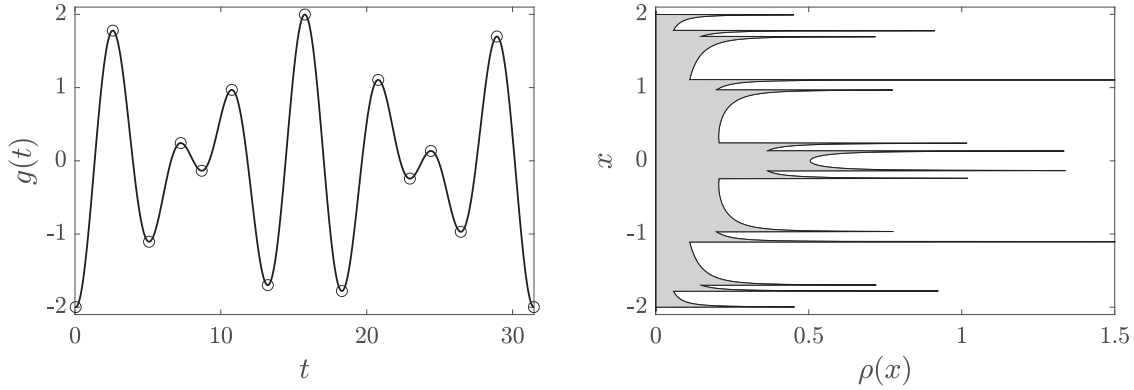

FIGURE 8 Periodic, biharmonic motion given by $g(t) = -\cos(t) - \cos(1.4t - 0.1)$ and its numerically obtained CPD.

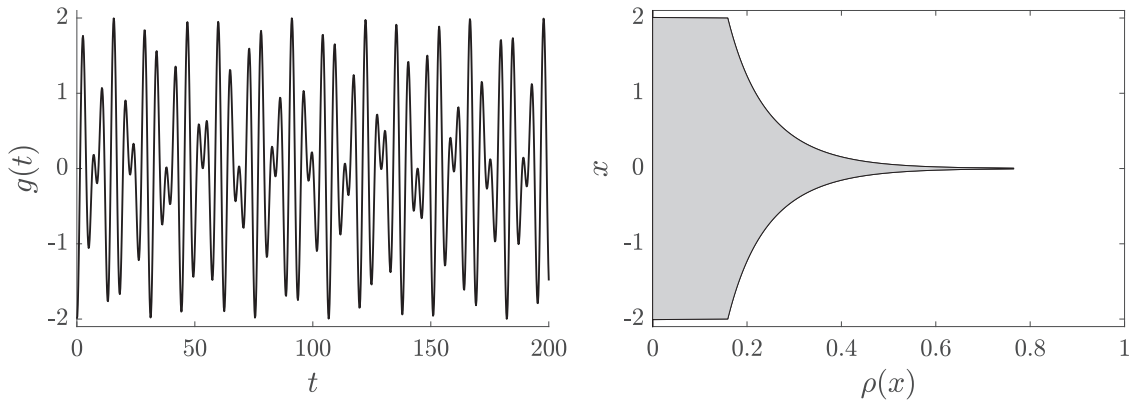

FIGURE 9 Aperiodic, biharmonic motion given by $g(t) = -\cos(t) - \cos(\sqrt{2}t - 0.1)$ and its analytically obtained CPD.

of the summands. The result is given by Equation (108).

$$\rho_{\mathrm{BHO}}(x) = \begin{cases} 0 & \text{for } x < -A_1 - A_2, \\ \frac{1}{\pi^2\sqrt{A_1 A_2}} K\left(\frac{(A_1+A_2)^2 - x^2}{4A_1A_2}\right) & \text{for } -A_1 - A_2 < x < -A_1 + A_2, \\ \frac{2}{\pi^2\sqrt{(A_1+A_2)^2 - x^2}} K\left(\frac{4A_1A_2}{(A_1+A_2)^2 - x^2}\right) & \text{for } -A_1 + A_2 < x < A_1 - A_2, \\ \frac{1}{\pi^2\sqrt{A_1 A_2}} K\left(\frac{(A_1+A_2)^2 - x^2}{4A_1A_2}\right) & \text{for } A_1 - A_2 < x < A_1 + A_2, \\ 0 & \text{for } A_1 + A_2 < x, \end{cases} \tag{108}$$

where $K(m)$ is the complete elliptic integral of the first kind with modulus m. For further details of the CPD's calculation, please refer to Appendix D.

If $g(t)$ is periodic, the frequency ratio can be written as $\omega_2/\omega_1 = a/b$ with $a, b \in \mathbb{N}$ being relative primes to each other. Thus, the time period is given by $\tau = 2\pi a/\omega_1$. The PDF of $g(t)$ depends strongly on the values of A_1, A_2, a, and b and the initial phase difference of the two harmonics $\beta_2 - \beta_1$. Since the sample necessary to describe the PDF has a finite length, at every turning point of $g(t)$ the PDF ρ has a singularity (cf. Figure 8). In contrast, for an aperiodic function, the sample has to be infinitely long, resulting in the limiting case with only one ($A_1 = A_2$) or two peaks ($A_1 \neq A_2$).

Figures 8 and 9 give examples of the CPD of a periodic biharmonic motion with $\omega_2/\omega_1 = 1.4$ and an aperiodic motion with $\omega_2/\omega_1 = \sqrt{2}$. The latter case is further analyzed and is represented in Figure 10a.

15214001, 0, Downloaded from https://onlinelibrary.wiley.com/doi/10.1002/zamm.202300432, Wiley Online Library on [23/03/2024]. See the Terms and Conditions (https://onlinelibrary.wiley.com/terms-and-conditions) on Wiley Online Library for rules of use; OA articles are governed by the applicable Creative Commons License

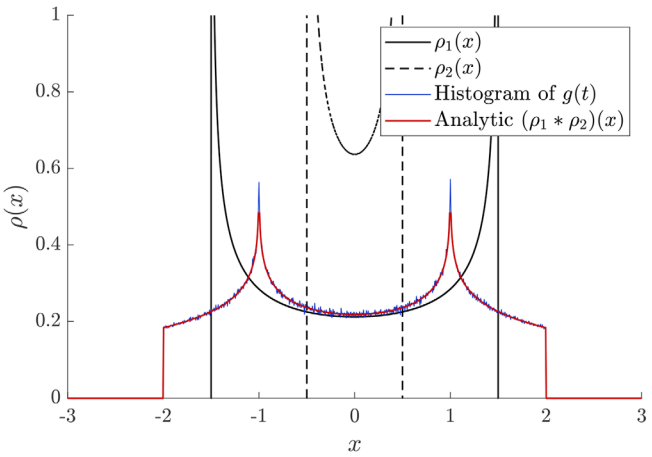

(a) CPD $\rho(x)$ of the quasi-periodic motion $g(t) = 1.5\sin(t) + 0.5\sin(\sqrt{2}t)$. The histogram-based numerical approximation (blue) is compared to the exact analytic solution (red). $\rho_1(x)$ and $\rho_2(x)$ represent the CPDs of the individual harmonics in $g(t)$

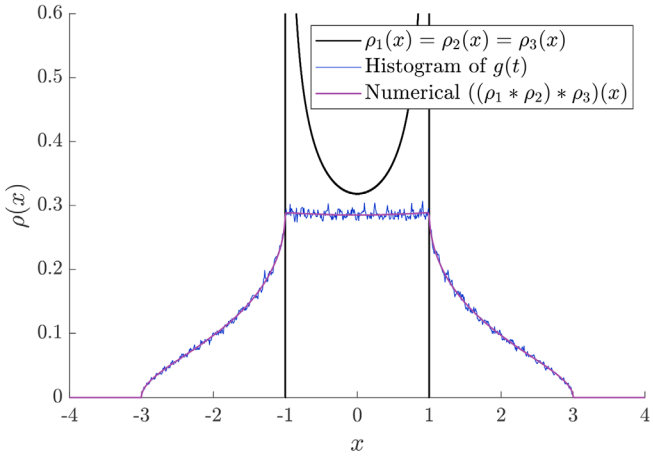

(b) CPD $\rho(x)$ of $g(t) = \sin(t)+\sin(\sqrt{2}t)+\sin(\sqrt{3}t)$. The black line represents the CPD of the individual harmonic terms, the arcsine distribution with half-width 1. The numerical estimate based on convolution is given in purple, while the histogram-based estimate is given in blue

FIGURE 10 CPD of polyharmonic functions. Two different numerical approaches are shown.

4 | NUMERICAL METHODS

If $g(t)$ is more complicated than in the above examples, the usage of numerical methods might become necessary since Equation (7) cannot be solved analytically anymore. The numerical approximation of the PDF is also necessary if $g(t)$ is not known explicitly but is only given as a numerical solution of an ODE. The following describes two general and one specific methods, highlighting their advantages and disadvantages.

4.1 | Histogram-based approximation of the CPD

Arguably, the simplest numerical method for obtaining $\rho(x)$ from $g(t)$ that instinctively comes to mind is based on sampling, that is, on constructing a histogram. $g(t)$ is evaluated at a large number of equidistantly placed values, and the obtained data are plotted in a histogram (cf. Figure 10) [32]. Subsequently, splines can be fitted on the data to evaluate the result at arbitrary values.

The histogram converges to the PDF [41] as the number of evaluation points tends to infinity. The advantage of the method is that it can be applied flexibly in long or short intervals, and the possibility of evaluating $g(t)$ (without explicitly having a formula for it) is sufficient. The convergence to the CPD depends mainly on the number of function evaluations.

The main disadvantage of the method is its relatively slow convergence.

4.2 | Spline-based approximation of the CPD

Once Equations (3) and (7) are known; instinctively, one considers the usage of splines (cf. Figure 8). Since we can only handle monotonically increasing or decreasing intervals, $g(t)$ has to be truncated into pieces $g_i(t)$ such that they are either monotonically increasing or decreasing. We can divide $g(t)$ at its local extrema to achieve this. Then, on each piece, $g_i(t)$ is evaluated at a sufficiently large number of points $x_{N_i} \in \mathbb{R}^{N_i}$, which do not necessarily have to be distributed equidistantly. After that, natural cubic splines are fitted to the data $(x_{N_i}, g_i(x_{N_i}))$.

Further on, the derivatives and inverses of these splines are needed. A straightforward way to get the derivative is to calculate it piecewise from the polynomial pieces of the splines. Fitting splines on the data $(g_i(x_{N_i}), x_{N_i})$ is a direct method to obtain the inverse. Spline fitting is performed easily using MATLAB™'s curve fitting tool. The fits are combined as

15214001, 0, Downloaded from https://onlinelibrary.wiley.com/doi/10.1002/zamm.202300432, Wiley Online Library on [23/03/2024]. See the Terms and Conditions (https://onlinelibrary.wiley.com/terms-and-conditions) on Wiley Online Library for rules of use; OA articles are governed by the applicable Creative Commons License

prescribed by Equation (3), and their weighted sum is calculated as given by Equation (7); thus, the result is a fit that can be evaluated at arbitrary values.

The advantage of the method is the more exact estimation of the CPD, even with relatively few spline nodes.

The disadvantage is that for nonperiodic, highly oscillating functions, the estimation of the CPD on long intervals can be very slow due to the large number of pieces created between local extrema of $g(t)$.

4.3 | Convolution-based approximation of the CPD for special cases

In special cases, when $g(t)$ is given by the sum of n independent functions $g_i(t)$ with $i = 1, \dots, n$ with individual CPDs $\rho_i(x)$, the resulting CPD $\rho(x)$ might be obtained by consecutive $n-1$ times numerical convolution of all $\rho_i(x)$ (cf. Figure 10b)[1]. To do so, the CPDs are evaluated at many equidistant points, and $n-1$ numerical convolutions are performed so that at the end all $\rho_i(x)$ are contained in the result. Since convolution is associative, it does not matter in which order the CPDs are convoluted with each other. Subsequently, splines are fitted to the data. At the same time, numerical quadrature is used to normalize the area under the fit to compensate for numerical inaccuracies.

The spline-based method is advantageous for periodic $g(t)$ with the known time period, whereas the histogram-based method is better suited for nonperiodic $g(t)$. In exceptional cases, the convolution-based method can obtain significantly more accurate results than the histogram-based method.

In any of the three presented methods, the final result is a fit that MATLAB can use just as any built-in function. However, keeping the number of data points within limits is essential since the evaluation time might increase unnecessarily.

4.4 | Numerical averaging

Once the CPD $\rho(x)$ is obtained in analytic or numerical form, the cross-correlation, described in Theorem 2, has to be calculated to obtain the average of $f(x_S + g(t))$. If analytically, the solution is not accessible by direct integration or Fourier transformation, a numerical one must be found.

Three basic approaches are given below.

1. Direct numerical quadrature of

$$\frac{1}{T}\int_0^T f(x_S + g(t))\mathrm{d}t \tag{109}$$

with N_x fixed values of x_S followed by subsequent spline fitting on the obtained data. The equidistant evaluation of $f(x_S + g(t))$ for many values of t ($t_i = 0, T/N_t, 2T/N_t, \dots, (N_t - 1)T/N_t$) and the calculation of their mean is the midpoint rule Riemann sum with $\Delta x = \text{const}$. It is well known that for sufficiently smooth (C^2) functions, this quadrature rule has a quadratic convergence rate, thus the mean average error (MAE), defined in Equation (117) is of $O(N_t^{-2})$ and is independent of the spatial resolution N_x (cf. Figure 11b). The computational cost is $O(N_t N_x)$. In Figure 11a, sublinear dependency on N_t and N_x can be observed based on a numerical experiment due to MATLAB's algorithm, which evaluates vector data structures sublinearly proportional to their size.

   The direct numerical quadrature approach is problematic if $T \to \infty$, and it can generally be slow since new function evaluations are needed for every new value of x_S.

   However, this is the only possible way if the target function to average is of the form $f(x_S, x_F, t)$.
2. Numerical computation of $(\rho \star f)(x_S)$. Much faster than the previous method since $f(x)$ does not have to be evaluated repeatedly. Instead, $\rho(x)$ has to be obtained. Once $f(x)$ and $\rho(x)$ are discretized at N_x equidistant grid points, their numerical cross-correlation can be performed. The numerical convolution of two vectors of length n_x is an operation of cost $O(N_x^2)$ when done by its definition.
3. Numerical cross-correlation, taking advantage of the properties of the Fourier transform, can be evaluated using the FFT with computational cost $O(N_x \log N_x)$, which is the most significant advantage of this method (cf. Figure 12a).

[1] By independent, we mean that $g(t)$ has the same CPD as the sum of the independent random variables X_i described by their PDFs $\rho_i(x)$.

15214001, 0, Downloaded from https://onlinelibrary.wiley.com/doi/10.1002/zamm.202300432, Wiley Online Library on [23/03/2024]. See the Terms and Conditions (https://onlinelibrary.wiley.com/terms-and-conditions) on Wiley Online Library for rules of use; OA articles are governed by the applicable Creative Commons License

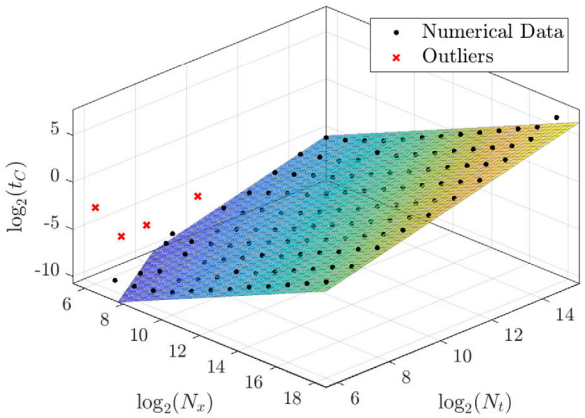

(a) $\log_2 t_C \approx -22 + 0.9411 \log_2 N_x + 0.7031 \log_2 N_t$ with $R^2 = 0.9888$

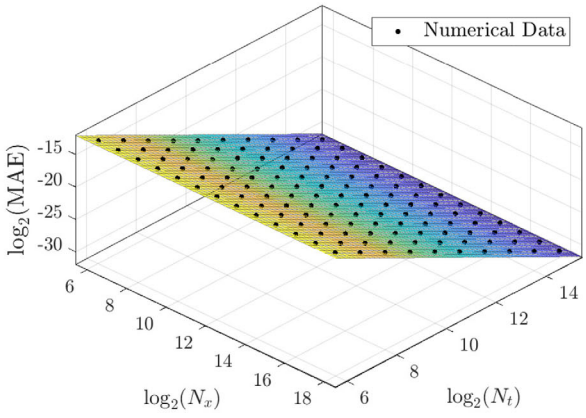

(b) $\log_2 \mathrm{MAE} \approx -0.9962 + 0.003 \log_2 N_x - 2 \log_2 N_t$ with $R^2 = 1$

FIGURE 11 Plane fits on the computational time t_C and the MAE represented against the spatial and temporal discretization resolution in a log-log plot.

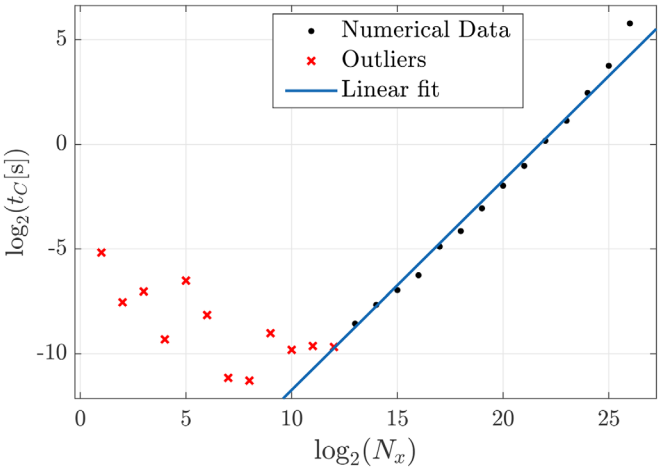

(a) Linear fit $\log_2 t_C \approx 0.9963 \log_2 N_x - 21.32$ with $R^2 = 0.9714$. $\mathcal{O}(N_x \log N_x)$ computational cost is expected

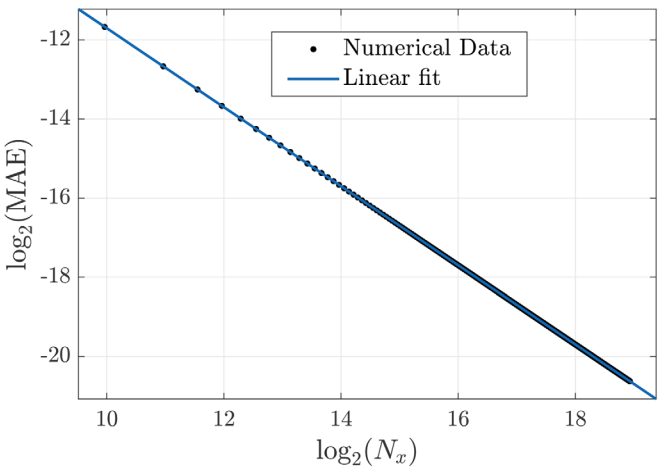

(b) Linear fit $\log_2 \mathrm{MAE} \approx -0.9999 \log_2 N_x - 1.701$ with $R^2 = 1$

FIGURE 12 Computational time t_C and mean absolute error (MAE) depicted against the spatial resolution of the discretization in a log-log plot.

Indeed, MATLAB's inbuilt cross-correlation function `xcorr` itself uses FFT. For sufficiently smooth $f(x)$ and bounded $\rho(x)$, the MAE of cross-correlation-based numerical averaging is inversely proportional to the discretization step length since the numerical quadrature, in this case, corresponds to a Riemann sum with the left rule, that is, $\mathrm{MAE} \sim N_x^{-1}$ (cf. Figure 12). If f or ρ are less regular, the convergence rate might be worse than linear (cf. Figure 13).

Example 4. The following shall demonstrate these properties using two benchmark examples with known analytic solutions. In the first case, let the "fast" motion be given by

$$g(t) = \frac{2A}{\pi} \arcsin \sin\left(\frac{\pi}{2}\omega t\right), \tag{110}$$

which is a triangle wave taking values between $-A$ and A and time period of $\tau = 4/\omega$, we assume $A < \pi$. It might be interpreted as the motion of a massless particle with energy $E_0 = A^2\omega^2$ in an "infinite well," that is, a PNO with $\alpha \to \infty$ of width $2A$.

15214001, 0, Downloaded from https://onlinelibrary.wiley.com/doi/10.1002/zamm.202300432, Wiley Online Library on [23/03/2024]. See the Terms and Conditions (https://onlinelibrary.wiley.com/terms-and-conditions) on Wiley Online Library for rules of use; OA articles are governed by the applicable Creative Commons License

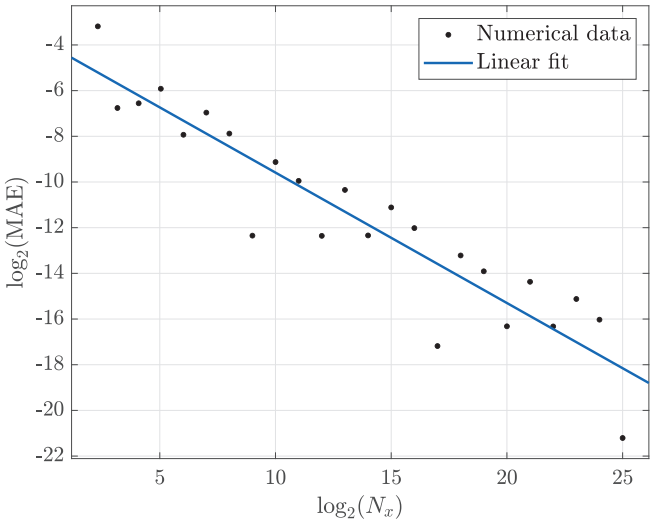

FIGURE 13 Linear fit $\log_2 \mathrm{MAE} \approx -0.5709 \log_2 N_x - 3.88$.

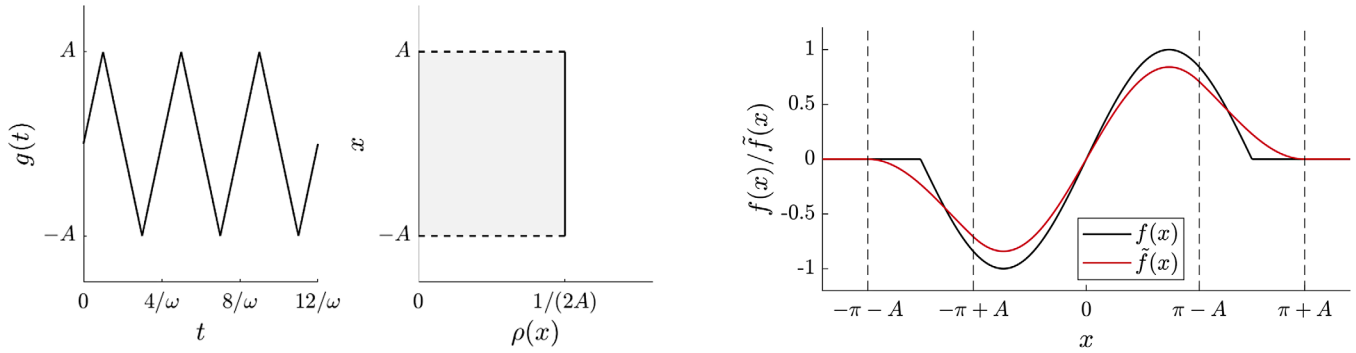

(a) Triangle wave function with amplitude A and its CPD

(b) $f(x)$ and its averaged values $\tilde{f}(x)$ with $A = 1$

FIGURE 14 Benchmark problem of averaging with a truncated sine and a triangle wave.

The target function $f(x)$ to be averaged will be a truncated sine force field given by

$$f(x) = \begin{cases} \sin x & \text{for } |x| < \pi, \\ 0 & \text{otherwise.} \end{cases} \tag{111}$$

The problem to be solved by averaging is

$$\tilde{f}(x) = \frac{\omega}{4} \int_0^{\frac{4}{\omega}} \sin\left(x + \frac{2A}{\pi} \arcsin \sin\left(\frac{\pi}{2}\omega t\right)\right) \mathbf{1}_{(-\pi,\pi)}\left(x + \frac{2A}{\pi} \arcsin \sin\left(\frac{\pi}{2}\omega t\right)\right) \mathrm{d}t. \tag{112}$$

The calculation of Equation (112) in this form is not trivial. However, the average can be easily obtained using Theorem 2. The CPD (cf. Figure 14a) is given by

$$\rho(x) = \begin{cases} \frac{1}{2A} & \text{for } |x| < A, \\ 0 & \text{otherwise,} \end{cases} \tag{113}$$

and so the average is determined by

$$\tilde{f}(x_S) = \int_{-\infty}^{\infty} g(x)\rho(x - x_S)\mathrm{d}x = \frac{1}{2A} \int_{-A+x_S}^{A+x_S} \sin x \, \mathbf{1}_{(-\pi,\pi)}(x)\mathrm{d}x. \tag{114}$$

15214001, 0, Downloaded from https://onlinelibrary.wiley.com/doi/10.1002/zamm.202300432, Wiley Online Library on [23/03/2024]. See the Terms and Conditions (https://onlinelibrary.wiley.com/terms-and-conditions) on Wiley Online Library for rules of use; OA articles are governed by the applicable Creative Commons License

The result will be piecewise defined; thus, we introduce the boundary points

$$d_1 = -\pi - A, \qquad d_2 = -\pi + A, \qquad d_3 = \pi - A, \qquad d_4 = \pi + A. \tag{115}$$

We denote the five intervals defined by $d_1, \dots, d_4$ as

$$D_1 = \{x \in \mathbb{R} | x \le d_1\}, \qquad D_i = \{x \in \mathbb{R} | d_{i-1} \le x < d_i\} \quad \text{for } i = 2 \dots 4, \qquad D_5 = \{x \in \mathbb{R} | d_4 \le x\}.$$

Evaluating the integrals in the different domains, we finally obtain

$$\tilde{f}(x_S) = \begin{cases} 0 & x_S \in D_1, \\ -\frac{1}{2A}(1 + \cos(x_S + A)) & x_S \in D_2, \\ \mathrm{si}(A) \sin x_S & x_S \in D_3, \\ \frac{1}{2A}(1 + \cos(x_S - A)) & x_S \in D_4, \\ 0 & x_S \in D_5, \end{cases} \tag{116}$$

with $\mathrm{si}(A) := \sin(x)/x$. This solution will be compared with the numerical ones, taking $A = 1$. For a graphical representation, refer to Figure 14b.

In Figure 11a, the computational cost of the direct numerical integration of Equation (109) by Riemann sums is depicted against the resolution of the spatial (N_x) and temporal (N_t) discretization in a log-log plot. The computational cost shows a sublinear dependency in N_x and N_t. In Figure 11b, a log-log plot depicts the numerical solution's MAE against N_x and N_t. The MAE is defined as

$$\mathrm{MAE} = \frac{\sum_{i=1}^{N} |\hat{X}_i - X_i|}{N}, \tag{117}$$

where $\hat{X}$ denotes the estimates, while X stands for the exact values. In the direct numerical quadrature of Equation (109), N_x practically does not affect accuracy, while the absolute error decreases quadratically with increasing temporal resolution.

In Figure 12, the computational cost and the MAE are depicted against the resolution of the spatial discretization on a log-log scale. Due to MATLAB's FFT-based cross-correlation algorithm, the computational cost grows only almost linearly with the problem size, while the MAE is inversely proportional to the spatial resolution.

The second benchmark example is given in Example 2, $A = 0.5$ is used for numerical calculations. This problem is more challenging numerically than the previous one since $f(x)$ is not continuous, and the CPD of the arcsine distribution has singularities at its boundaries. However, the MAE converges to zero when the resolution of the spatial discretization tends to infinity (cf. Figure 13). The MAE is not evenly distributed: it becomes the largest at the domain boundaries due to the discontinuities of $f(x)$ (cf. Figure 2).

Example 5. A further numerical example is given to demonstrate the use of histogram-based averaging. Consider the problem of a strongly coupled pair of particles in a quadratic truncated potential well under harmonic high-frequency excitation as described in Ref. [42]. Assume that we only have the numerical simulation data $(x_{1,i}, x_{2,i}, t_i)$ for $i = 1, \dots, N$ with N denoting the number of samples corresponding to the following mechanical system.

$$m_1 \ddot{x}_1 + k(\dot{x}_1 - \dot{x}_2) + c(x_1 - x_2) + m_1 V'(x_1) = F \cos(\Omega t), \tag{118}$$

$$m_2 \ddot{x}_2 + k(\dot{x}_2 - \dot{x}_1) + c(x_2 - x_1) + m_2 V'(x_2) = 0, \tag{119}$$

$$x_1(0) = x_2(0) = x_0, \tag{120}$$

$$\dot{x}_1(0) = \dot{x}_2(0) = u_0, \tag{121}$$

with masses m_1 and m_2, damping coefficient k, spring stiffness c, excitation amplitude F, and angular frequency Ω. Furthermore, the particles underlie the force of a mass-proportional potential $m_i V(x_i)$ with $i \in \{1, 2\}$, where $V'(x) = x\mathbf{1}_{|x|<1}(x)$, and $\mathbf{1}_X(x)$ denotes the indicator function of the set X. In the numerical simulation, the nondimensional

15214001, 0, Downloaded from https://onlinelibrary.wiley.com/doi/10.1002/zamm.202300432, Wiley Online Library on [23/03/2024]. See the Terms and Conditions (https://onlinelibrary.wiley.com/terms-and-conditions) on Wiley Online Library for rules of use; OA articles are governed by the applicable Creative Commons License

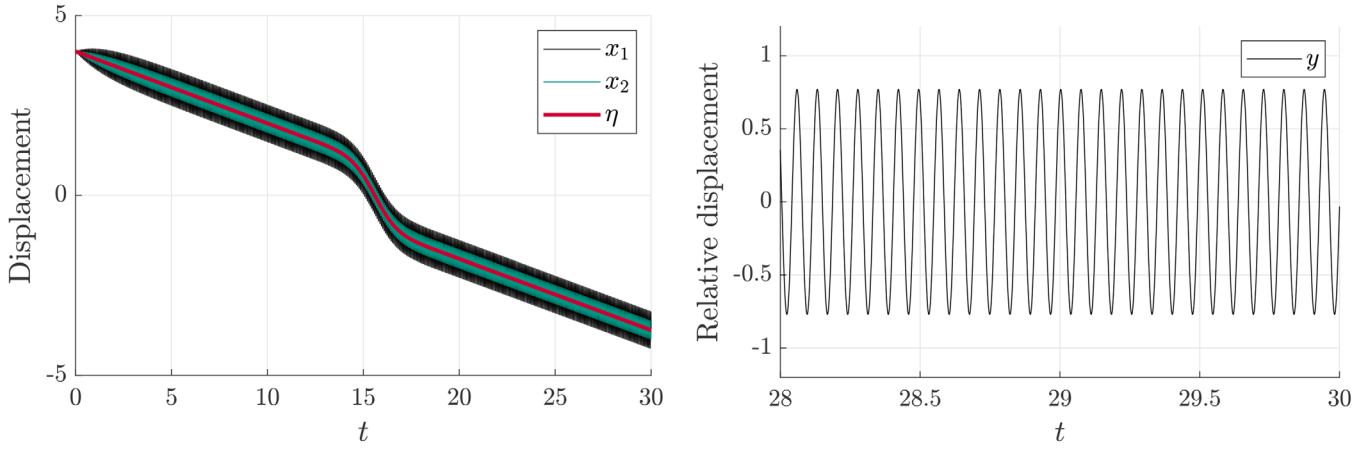

(a) Particle displacement and center of mass location

(b) Steady-state relative displacement $y_{st}(t)$

FIGURE 15 Temporal evolution of the system dynamics with parameters and initial conditions specified in the main text. It is noteworthy that the relative displacement quickly reaches a steady-state motion with constant amplitude, which is hardly affected when the particles move into the interior of the potential at $-1 < x_i < 1$ for $i \in \{1, 2\}$.

parameter and initial condition values are chosen as

$$m_1 = 1, \quad m_2 = 2, \quad k = 1, \quad c = 5000, \quad F = 100, \quad \Omega = \sqrt{\frac{c}{m} + 1 - \frac{k^2}{2m^2}} = 86.6018, \quad x_0 = 4, \quad u_0 = -0.2, \tag{122}$$

that is, the particle starts its motion outside the potential well but moves towards it. Ω is chosen so that the most resonant frequency of the particle chain is excited [42]. In this example, we assume that we know nothing about the excitation or the system parameters except the knowledge of the restoring force $V'(x)$ and the masses m_1 and m_2. When plotting the numerical data (cf. Figure 15) we recognize a "slow-fast" system dynamics. Although large-amplitude oscillations can be caused in the relative displacement with the given parameter values, the decay of "fast" transients is still quick compared to the "slow" system's dynamics. Thus, the system has the form of Equations (100)–(102). Our goal is to identify the underlying "slow" dynamics of the system based on our limited knowledge. After introducing two new parameters,

$$\frac{1}{m} := \frac{1}{m_1} + \frac{1}{m_2} \quad \text{and} \quad \mu = \frac{m_1}{m_1 + m_2}, \tag{123}$$

we can apply a coordinate transform to separate the "slow" and "fast" dynamics from each other. Separation can be achieved by defining the following quantities:

$$\eta = \mu m_1 + (1 - \mu) m_2, \quad \text{and} \quad y = x_2 - x_1, \tag{124}$$

Here, η represents the displacement of the center of mass, while y represents the relative displacement of the particles.

The "fast" dynamics rapidly reaches a steady-state, constant-amplitude vibration, which we denote with $y_{st}(t)$. Furthermore, it is clear that the particles' center of mass is predominantly "slow" and has only a negligible, small-amplitude "fast" oscillation. Nevertheless, its "slow" dynamics is different from that of a single free particle traversing the potential under identical initial conditions, since the "fast" oscillations affect the "slow" dynamics. The differential equation of the center of mass is given by

$$\ddot{\eta} + \mu V'(\eta + z_1(t)) + (1 - \mu) V'(\eta + z_2(t)) = \mu F \cos(\Omega t), \tag{125}$$

$$\eta(0) = x_0, \tag{126}$$

$$\dot{\eta}(0) = u_0, \tag{127}$$

15214001, 0, Downloaded from https://onlinelibrary.wiley.com/doi/10.1002/zamm.202300432, Wiley Online Library on [23/03/2024]. See the Terms and Conditions (https://onlinelibrary.wiley.com/terms-and-conditions) on Wiley Online Library for rules of use; OA articles are governed by the applicable Creative Commons License

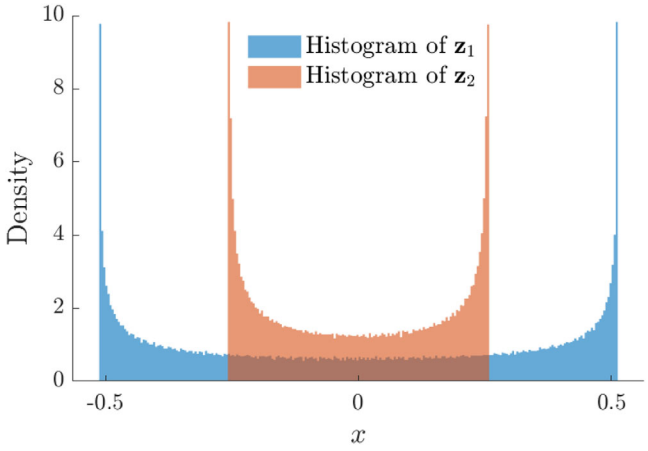

FIGURE 16 Histogram of the particles displacement data $\mathbf{z}_1, \mathbf{z}_2$ centered around $\boldsymbol{\eta}$. Although the linear function interpolation on the histogram does not yield a smooth function, it is not a problem when calculating the cross-correlation-based average.

with the "fast" variables

$$z_1(t) = -(1-\mu)y_{\mathrm{st}}(t) \quad \text{and} \quad z_2(t) = \mu y_{\mathrm{st}}(t). \tag{128}$$

Proceeding analytically would involve the averaging of Equation (125). By introducing $\xi = \langle \eta \rangle$, we can write this average as

$$\ddot{\xi} + \underbrace{\mu V'_{\mathrm{eff},1}(\xi) + (1-\mu)V'_{\mathrm{eff},2}(\xi)}_{V'_{\mathrm{eff}}(\xi) :=} = 0, \tag{129}$$

$$\xi(0) = x_0, \tag{130}$$

$$\dot{\xi}(0) = u_0, \tag{131}$$

with $V'_{\mathrm{eff},1}(\xi) = \left\langle V'(\eta + z_1(t)) \right\rangle$ and $V'_{\mathrm{eff},2}(\xi) = \left\langle V'(\eta + z_2(t)) \right\rangle$. For brevity, we introduce their weighted sum $V'_{\mathrm{eff}}(\xi)$ as defined in Equation (129).

In practice, we work with discrete numerical data. Thus, only the data points $z_{j,i} = z_j(t_i)$ with $i = 1, \ldots, N$ and $j \in \{1, 2\}$ are available. We select the values of the data vectors $\mathbf{z}_{1,\mathrm{st}}$ and $\mathbf{z}_{2,\mathrm{st}}$ for which the transients in the relative displacement have sufficiently decayed and build the histograms $\boldsymbol{\rho}_1$ and $\boldsymbol{\rho}_2$ of the data vectors (see Figure 16). Linear interpolants are fitted to the histograms, resulting in the functions $\rho_1(x)$ and $\rho_2(x)$. These can be combined in a resulting CPD given by $\rho(x) = \mu\rho(x)_1 + (1-\mu)\rho(x)_2$. Now, the procedure described in Section 4.4 Point 3., can be applied to obtain the effective potential. In the region of interest $(x_{\min}, x_{\max}) = (-2, 2)$, an equidistant grid $\mathbf{x}_{\mathrm{grid}}$ is generated containing N_x number of grid points. After evaluating $\mathbf{V}' = V'(\mathbf{x}_{\mathrm{grid}})$ and $\boldsymbol{\rho} = \rho(\mathbf{x}_{\mathrm{grid}})$ on the same grid, we can obtain the discretized effective potential by calculating

$$\mathbf{V}'_{\mathrm{eff}} = \mathrm{IFFT}\Big(\mathrm{FFT}(\mathbf{V}') \circ \overline{\mathrm{FFT}(\boldsymbol{\rho})}\Big), \tag{132}$$

where FFT and IFFT denote the fast Fourier transform and its inverse, whereas $\mathbf{v} \circ \mathbf{u}$ denotes the Hadamard product, that is, the element-wise multiplication of vectors $\mathbf{v}$ and $\mathbf{u}$. Finally, using interpolation through the data points of $\mathbf{V}'_{\mathrm{eff}}$, we create a MATLAB object $V'_{\mathrm{eff}}(\xi)$ that can be used as a function in possible further calculations. The results are shown in Figure 17.

Verifying our calculations by estimating the "slow" dynamics using other methods is possible. As there is no damping, the motion of the center of mass can be compared with that of a free particle in a conservative potential after applying a low-pass filter, which allows us to estimate the restoring force simply by $V'_{\mathrm{acc}}(\eta) \approx -\ddot{\eta}_{\mathrm{LP}}$, with the derivative of the low-pass-filtered position of the center of mass being evaluated numerically. The graphical representation of this validation is also shown in Figure 17, which shows good agreement between the two different estimates. It is important to note

15214001, 0, Downloaded from https://onlinelibrary.wiley.com/doi/10.1002/zamm.202300432, Wiley Online Library on [23/03/2024]. See the Terms and Conditions (https://onlinelibrary.wiley.com/terms-and-conditions) on Wiley Online Library for rules of use; OA articles are governed by the applicable Creative Commons License

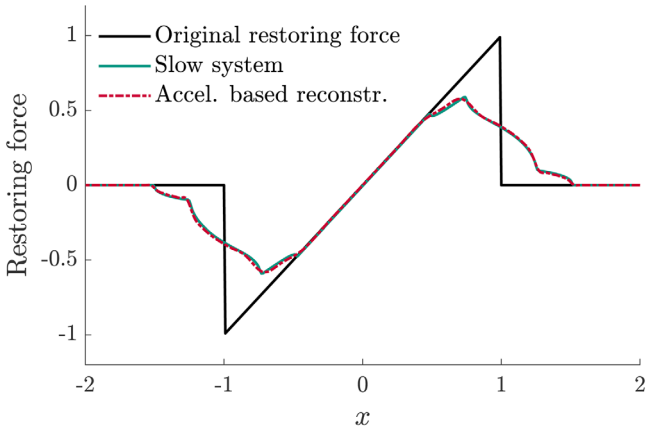

FIGURE 17 Original restoring force $V'(x)$ (with black) and the numerically calculated effective restoring force $V'_{\text{eff}}(x)$ with green, as well as the acceleration-based estimate of the effective force $V'_{\text{acc}}(x)$ with red.

that, without low-pass filtering, the numerical derivatives are too noisy to provide a usable estimate. However, low-pass filtering smooths out sharp edges that are expected to appear in the effective restoring force. Indeed, the more accurate cross-correlation-based estimate retains these details of the "slow" dynamics.

5 | CONCLUSIONS

An efficient alternative to standard averaging based on cross-correlation has been proposed in this article. The method is applicable if the dependent variable can be written as the sum of a "slow" and a "fast" variable, which is often the case since various methods of nonlinear dynamics, like multiple scales, averaging, or Blekhman's direct separation of motions are explicitly based on this assumption. In order to perform averaging on a function with the above "slow-fast" variable in its argument, it is sufficient if the CPD of the "fast" variable is known; its explicit time dependency itself is not required, although often available and may be used to obtain the CPD itself. In some cases, this might be a significant advantage over the classical way of evaluating the integral in Equation (109) since $g(t)$ does not have to be explicitly known. This fact provides an additional understanding of the concept of averaging. Information on the exact time history of the "fast" variable is discarded, and only the probability of its location is used.

A further alternative for the representation of averages of analytic functions has been provided by a specific type of expansion where the moments of the "fast" variable's CPD and the target function's derivatives are used. By utilizing the moment generating and characteristic functions of random variables, it is possible to perform averaging with "fast" variables with the same CDP as the sum of independent random variables. It is well known that the PDF of such random variables can be calculated by the convolution of the individual PDFs, which simplifies the product of their moment-generating/characteristic functions.

Furthermore, several explicit formulas for CPDs have been derived in this study, and how they might be utilized to perform averaging on piecewise defined polynomials has been shown. An efficient, FFT-based numerical method has been proposed for other analytically inaccessible cases.

The cross-correlation-based averaging method can be extended for the case of more than one dependent variable. However, it might be disadvantageous for periodic motions since in more than one spatial dimension, the CPD is not a function anymore, but it degenerates to a distribution on a set with zero measure, yet with unit hyper-volume. Still, for aperiodic motions, such as, for example, the motion of an undamped particle tossed in 45° angle in a two-dimensional rectangular "infinite well" with incommensurable side length (ideally elastic ball in billiard table), the CPD becomes a function, and the multidimensional cross-correlation can be calculated. In this case, the particle is found at any point of the potential well with the same constant velocity inversely proportional to the area of the well.

We aim to attract the reader's attention to the model reduction technique proposed in this paper. The method has several potential applications in areas of science where multiple time scales are present. In fact, without proving the validity of the equivalence, the method has been used in previous research by the authors [42, 43] to reduce the complexity of the underlying escape problems, respectively.

15214001, 0, Downloaded from https://onlinelibrary.wiley.com/doi/10.1002/zamm.202300432, Wiley Online Library on [23/03/2024]. See the Terms and Conditions (https://onlinelibrary.wiley.com/terms-and-conditions) on Wiley Online Library for rules of use; OA articles are governed by the applicable Creative Commons License

One of the most interesting potential applications is when the CPD can be measured experimentally. In many cases, obtaining the high-frequency compound of the motion may be very difficult because fast, high-resolution measuring equipment is required. On the other hand, the CPD can be easily obtained as a "cloud" picture, approximating the linger time by the brightness. The CPD can be estimated and used with appropriate image processing to obtain the semi-empirical equations governing the "slow" system's evolution.

It may be an exciting hint for future work to build a potential bridge between the classical dynamics of high-frequency excited systems and quantum mechanics. Further applications are in the development of control strategies [44].

Future research might also consider finding other cases of motion where explicit CPDs can be derived. Investigating the goodness of approximations of CPDs, for example, through polynomials, might also be a direction for further research.

A possible generalization of this paper's results includes the extension of the cross-correlation integral to stochastic "fast" motions: Would the result on the equivalency of the time integral with a spatial cross-correlation hold in the stochastic case as well? If so, Theorem 2 may also be interpreted in the framework of the ergodic theory: a function's time average is exchanged by its spatial average.

ACKNOWLEDGMENTS

We thank PD Gudrun Thäter for proofreading this paper. Her assistance helped to refine and improve the quality of this work. This study was funded by the Deutsche Forschungsgemeinschaft (DFG, German Research Foundation) under Project No. 508244284. We are grateful for this financial support.

Open access funding enabled and organized by Projekt DEAL.

CONFLICT OF INTEREST STATEMENT

The authors declare no conflicts of interest.

ORCID

Attila Genda https://orcid.org/0000-0001-8061-8473

REFERENCES

[1] Landau, L.D., Lifshitz, E.M.: Mechanics, 3rd edn. Butterworth, Oxford (1976)
[2] Eckhaus, W.: New approach to the asymptotic theory of nonlinear oscillations and wave-propagation. J. Math. Anal. Appl. 49(3), 575–611 (1975)
[3] Gendelman, O.V.: Escape of a harmonically forced particle from an infinite-range potential well: a transient resonance. Nonlinear Dyn. 93(1), 79–88 (2018)
[4] Arnold, V.I., Kozlov, V.V., Neishtadt, A.I.: Mathematical Aspects of Classical and Celestial Mechanics. Encyclopaedia of Mathematical Sciences, 3rd edn. Springer Berlin, Heidelberg (2006). Original Russian edition published by URSS, Moscow, 2002.
[5] Fidlin, A., Drozdetskaya, O.: On the averaging in strongly damped systems: the general approach and its application to asymptotic analysis of the sommerfeld effect. Procedia IUTAM 19, 43–52 (2016)
[6] Aramendiz, J., Fidlin, A., Lei, K.: Investigations on amplitude adaptive sequential friction-spring dampers. ZAMM - J. Appl. Math. Mech./Zeitschrift für Angewandte Mathematik und Mechanik 101(7), e201800293 (2021)
[7] Schröders, S., Fidlin, A.: Asymptotic analysis of self-excited and forced vibrations of a self-regulating pressure control valve. Nonlinear Dyn. 103(3), 2315–2327 (2021)
[8] Guckenheimer, J., Holmes, P.: Nonlinear Oscillations Dynamical Systems and Bifurcations of Vector Fields. Springer-Verlag, Berlin (1990)
[9] Ballif, G., Clément, F., Yvinec, R.: Averaging of a stochastic slow-fast model for population dynamics: application to the development of ovarian follicles. SIAM J. Appl. Math. 82(1), 359–380 (2022)
[10] Krylov, N.M., Bogoliubov, N.N.: New Methods of Nonlinear Mechanics in their Application to the Investigation of the Operation of Electronic Generators, I (in Russian). United Scientific and Technical Press, Moscow (1934)
[11] Bogolyubov, N., Mitropolskii, Y.A.: Asymptotic Methods in the Theory of Nonlinear Oscillations. Foreign Technology Div Wright-Patterson AFB, Ohio (1955)
[12] Oliveira, A.R.E.: History of Krylov-Bogoliubov-Mitropolsky methods of nonlinear oscillations. Adv. Hist. Stud. 6, 40–55 (2017)
[13] Strygin, V.: On a modification of the averaging method for seeking higher approximations. J. Appl. Math. Mech. 48, 767–769 (1984)
[14] Khasminski, R.: On the avaraging principle for Ito stochastic differential equations. Kybernetika 4(3), 260–279 (1968)
[15] Liu, Z.H., Zhu, W.Q.: Stochastic averaging of quasi-integrable Hamiltonian systems with delayed feedback control. J. Sound Vib. 299(1), 178–195 (2007)
[16] Chen, L., Liang, X., Zhu, W., et al.: Stochastic averaging technique for SDOF strongly nonlinear systems with delayed feedback fractional-order PD controller. Sci. China Technol. Sci. 62, 287–297 (2019)
[17] Kifer, Y.: Some recent advances in averaging. In: Modern Dynamical Systems and Applications, pp. 385–403. Cambridge University Press, Cambridge (2004)

15214001, 0, Downloaded from https://onlinelibrary.wiley.com/doi/10.1002/zamm.202300432, Wiley Online Library on [23/03/2024]. See the Terms and Conditions (https://onlinelibrary.wiley.com/terms-and-conditions) on Wiley Online Library for rules of use; OA articles are governed by the applicable Creative Commons License

[18] Kifer, Y.: Averaging in dynamical systems and large deviations. Invent. Math. 110(1), 337–370 (1992)
[19] Kifer, Y.: Averaging principle for fully coupled dynamical systems and large deviations. Ergod. Theory Dyn. Syst. 24(3), 847–871 (2004)
[20] Volosov, V.M.: Averaging in systems of ordinary differential equations. Russ. Math. Surv. 17(6), 1 (1962)
[21] Guckenheimer, J., Holmes, P.: Averaging and Perturbation from a Geometric Viewpoint, pp. 166–226. Springer New York, New York, NY (1983)
[22] Mitropolskii, Y.A., Van Dao, N.: Averaging Method, pp. 282–326. Springer Netherlands, Dordrecht (1997)
[23] Sanders, J.A., Verhulst, F., Murdock, J.: Averaging Methods in Nonlinear Dynamical Systems. Applied Mathematical Sciences. Springer, New York (2007)
[24] Fidlin, A.: Nonlinear Oscillations in Mechanical Engineering. Springer Science & Business Media, Berlin (2005)
[25] Krein, P.T., Bentsman, J., Bass, R.M., Lesieutre, B.L.: On the use of averaging for the analysis of power electronic systems. IEEE Trans. Power Electron. 5(2), 182–190 (1990)
[26] Sun, J., Grotstollen, H.: Symbolic analysis methods for averaged modeling of switching power converters. IEEE Trans. Power Electron. 12(3), 537–546 (1997)
[27] Kifer, Y.: Averaging and climate models. In: Imkeller, P., von Storch, J.S. (eds.) Stochastic Climate Models, pp. 171–188. Birkhäuser Basel, Basel (2001)
[28] Hairer, E., Lubich, C., Wanner, G.: Geometric Numerical Integration. Structure-preserving Algorithms for Ordinary Differential Equations. Springer Series in Computational Mathematics, vol. 31, 2nd edn. Springer-Verlag, Berlin (2006)
[29] Leimkuhler, B., Reich, S.: A reversible averaging integrator for multiple time-scale dynamics. J. Comput. Phys. 171(1), 95–114 (2001)
[30] Makarov, B., Podkorytov, A.: Real Analysis: Measures, Integrals and Applications, pp. 244. Springer, London (2013). formula (2)
[31] Griffiths, D.J., Schroeter, D.F.: Introduction to Quantum Mechanics. Cambridge University Press, Cambridge (2018)
[32] Robinett, R.W.: Quantum and classical probability distributions for position and momentum. Am. J. Phys. 63(9), 823–833 (1995)
[33] Real, C.C., Muga, J.G., Brouard, S.: Comment on "Quantum and classical probability distributions for position and momentum," by R. W. Robinett [Am. J. Phys. 63 (9), 823–832 (1995)]. Am. J. Phys. 65(2), 157–158 (1997). https://doi.org/10.1119/1.18791
[34] Yoder, G.: Using classical probability functions to illuminate the relation between classical and quantum physics. Am. J. Phys. 74(5), 404 (2006)
[35] Devore, J.L., Berk, K.N.: Modern Mathematical Statistics with Applications. Springer Texts in Statistics, 2nd edn. Springer New York, NY (2012)
[36] Kendall, M.G., Stuart, A., Ord, J.K.: Kendall's Advanced Theory of Statistics, Distribution Theory, vol. 1, 6th edn. John Wiley & Sons, Chichester (1994)
[37] Lyapunov, A.M.: Stability of Motion. GITTL, Moscow (1950)
[38] Gelb, A., Vander Velde, W.E.: Multiple-Input Describing Functions and Nonlinear System Design. McGraw-Hill, New York (1968)
[39] Nayfeh, A.H., Mook, D.T.: Nonlinear Oscillations. Wiley, New York (1979)
[40] Kovacic, I.: Nonlinear Oscillations: Exact Solutions and their Approximations, 1st edn. Springer Cham, Switzerland (2020), Hardcover ISBN: 978-3-030-53171-3; Softcover ISBN: 978-3-030-53174-4; eBook ISBN: 978-3-030-53172-0.
[41] Hogg, R.V., McKean, J.W., Craig, A.T.: Introduction to Mathematical Statistics, 6th edn. Prentice Hall, Upper Saddle River, New Jersey (2004)
[42] Genda, A., Fidlin, A., Gendelman, O.: On the escape of a resonantly excited couple of particles from a potential well. Nonlinear Dyn. 104(1), 91–102 (2021)
[43] Genda, A., Fidlin, A., Gendelman, O.: On the escape of a resonantly excited couple of colliding particles from a potential well under bi-harmonic excitation. In: 10th European Nonlinear Dynamics Conference (ENOC 2022), Lyon, Frankreich, 17-22 July 2022 . https://enoc2020.sciencesconf.org/375919/document
[44] Fidlin, A., Juel Thomsen, J.: Non-trivial effects of high-frequency excitation for strongly damped mechanical systems. Int. J. Non Linear Mech. 43(7), 569–578 (2008)
[45] Bronstein, I., Semendjajew, K., Musiol, G., Mühlig, H.: Taschenbuch der Mathematik. Verlag Harri Deutsch, Frankfurt am Main (2001)
[46] Bateman, H.: Higher Transcendental Functions [Volumes I-III], vol. I-III. McGraw-Hill Book Company, New York (1953)

How to cite this article: Genda, A., Fidlin, A., Gendelman, O.: An alternative approach to averaging in nonlinear systems using classical probability density. Z Angew Math Mech. e202300432 (2024). https://doi.org/10.1002/zamm.202300432

APPENDIX A: MOMENTS OF THE ARCSINE DISTRIBUTION

The arcsine distribution's moments and partial moments are obtained in the following. First, the moment-generating function $M_X(t)$ of the standard arcsine distribution (a special case of the Beta distribution with parameters $\alpha = \beta = 1/2$), given in (0,1) is derived. Let $X \sim \text{Beta}(1/2, 1/2)$ be a random variable following the standard arcsine distribution, of which

15214001, 0, Downloaded from https://onlinelibrary.wiley.com/doi/10.1002/zamm.202300432, Wiley Online Library on [23/03/2024]. See the Terms and Conditions (https://onlinelibrary.wiley.com/terms-and-conditions) on Wiley Online Library for rules of use; OA articles are governed by the applicable Creative Commons License

the moment-generating function is defined as

$$M_X(t) = \mathrm{E}\left[e^{tX}\right] = \int_0^1 e^{tx} \frac{1}{\pi\sqrt{x(1-x)}} \mathrm{d}x = {}_1F_1\left(\frac{1}{2}; 1; t\right), \tag{A1}$$

where ${}_1F_1\,(a; b; t)$ denotes the confluent hypergeometric function defined by

$${}_1F_1(a; b; t) = \frac{\Gamma(b)}{\Gamma(a)\Gamma(b-a)} \int_0^1 e^{tu} u^{a-1}(1-u)^{b-a-1} \mathrm{d}u. \tag{A2}$$

By a linear transformation, the distribution's location and scaling can be changed, that is,, by $Y = \alpha X + \beta$, the random variable is shifted to the negative direction by β and stretched by α. The moment-generating function then becomes

$$M_{\alpha X+\beta}(t) = \mathrm{E}\left[e^{(\alpha X+\beta)t}\right] = e^{\beta}\mathrm{E}\left[e^{\alpha X t}\right] = e^{\beta t} M_X(\alpha t) = e^{\beta t}\, {}_1F_1\left(\frac{1}{2}, 1, \alpha t\right) = \exp\left(\frac{\alpha t}{2} + \beta t\right) I_0\left(\frac{\alpha z}{2}\right), \tag{A3}$$

with $I_0(x)$ denoting the modified Bessel function of the first kind of the zeroth order. The moments are given by

$$m_n = M^{(n)}_{\alpha X+\beta}(t)\big|_{t=0}. \tag{A4}$$

For the confluent hypergeometric function, the following identity holds.

$$\frac{\mathrm{d}^k}{\mathrm{d}t^k} {}_1F_1(a, b, t) = \frac{(a)_k}{(b)_k} {}_1F_1(a + k, b + k, t), \tag{A5}$$

where $(a)_k$ denotes the rising factorial, that is, $(a)_k = a(a + 1)(a + 2)\ldots(x + k - 1)$ and $(a)_0 = 1$. By making use of the identity, one obtains the k^{th} derivative of Equation (A3)

$$M^{(k)}_{\alpha X+\beta}(t) = \sum_{j=0}^{k} \binom{k}{j} \alpha^j \beta^{k-j} \frac{\left(\frac{1}{2}\right)_j}{(1)_j} e^{\beta t}\, {}_1F_1\left(\frac{1}{2} + j, 1 + j, \alpha t\right). \tag{A6}$$

Inserting $t = 0$, one obtains the moments

$$m_k = \sum_{j=0}^{k} \binom{k}{j} \alpha^j \beta^{k-j} \frac{\left(\frac{1}{2}\right)_j}{(1)_j} = \beta^k + \sum_{j=1}^{k} \binom{k}{j} \alpha^j \beta^{k-j} \frac{(2j-1)!!}{2^j j!}, \quad \text{for } k \geq 1. \tag{A7}$$

where $(2j - 1)!! = (2j - 1)(2j - 3)\ldots 3 \cdot 1$ is the double factorial. In case of a centered arcsine distribution with $\alpha = 2A$ and $\beta = -A$, one has

$$m_k = A^k \left((-1)^k + \sum_{j=1}^{k} \binom{k}{j} (-1)^{k-j} \frac{(2j-1)!!}{j!}\right) = \begin{cases} A^k \frac{1}{2^k} \binom{k}{k/2} & \text{for } k \text{ even}, \\ 0 & \text{for } k \text{ odd}, \end{cases} \quad \text{for } k \geq 1. \tag{A8}$$

The partial moments of the centered arcsine distribution can be determined by solving the integral

$$m_k(x; A) = \int_{-A}^{x} \frac{y^k}{\pi\sqrt{A^2 - y^2}} \mathrm{d}y = A^k \int_{-\frac{\pi}{2}}^{\arcsin\frac{x}{A}} \sin^k t \mathrm{d}t, \tag{A9}$$

where the change of variables $y = A \sin t$ has been applied. The indefinite integral of $\sin^k t$ can be obtained by using recursively the identity [45]

$$\int \sin^k t \mathrm{d}t = -\frac{\sin^{k-1} t \cos t}{k} + \frac{k-1}{k} \int \sin^{k-2} t \mathrm{d}t. \tag{A10}$$

15214001, 0, Downloaded from https://onlinelibrary.wiley.com/doi/10.1002/zamm.202300432, Wiley Online Library on [23/03/2024]. See the Terms and Conditions (https://onlinelibrary.wiley.com/terms-and-conditions) on Wiley Online Library for rules of use; OA articles are governed by the applicable Creative Commons License

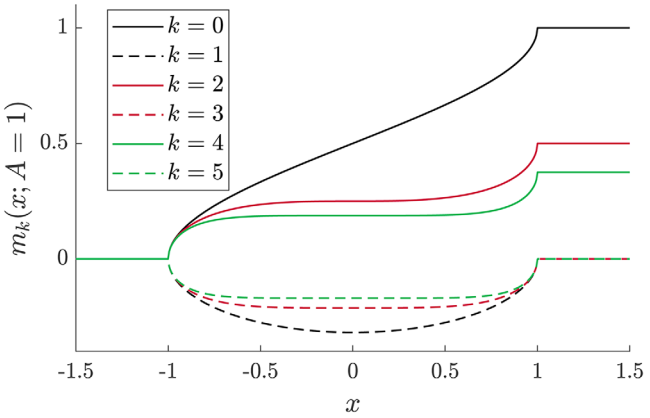

FIGURE A1 Partial moments of the arcsine distribution with $A = 1$.

Thus,

$$\int \sin^k t\,\mathrm{d}t = \begin{cases} -\cos t\left(\sum_{j=0}^{\frac{k-1}{2}} p(k,j)\sin^{k-2j-1} t\right) & \text{for } k \text{ even}, \\ -\cos t\left(\sum_{j=0}^{\frac{k}{2}-1} p(k,j)\sin^{k-2j-1} t\right) + p(k,\tfrac{k}{2}-1)t & \text{for } k \text{ odd}. \end{cases} \tag{A11}$$

with

$$p(k,j) = \begin{cases} \dfrac{\binom{k}{k/2}}{2^{2j+2}(k-2j-1)\binom{k-1-2j}{(k-1)/2-j}} & \text{for } k \text{ even}, \\ \dfrac{2^{2j}\binom{k-2j-1}{(k-1)/2}}{\binom{k-1}{(k-1)/2}k} & \text{for } k \text{ odd}. \end{cases} \tag{A12}$$

Hence, Equation (A9) becomes

$$m_k(x;A) = \begin{cases} 0 & \text{for } x < -A \\ -\pi^{-1}\sqrt{A^2-x^2}A^{k-1}\sum_{j=0}^{(k-1)/2} p(k,j)x^{k-2l-1} & \text{for } |x| < A \text{ and } k \text{ even}, \\ -\pi^{-1}\sqrt{A^2-x^2}A^{k-1}\sum_{j=0}^{k/2-1} p(k,j)x^{k-2l-1} + p(k,k/2-1)\left(\pi^{-1}\arcsin(x/A)+1/2\right) & \text{for } |x| \le A \text{ and } k \text{ odd}, \\ m_k & \text{for } A < x, \end{cases} \tag{A13}$$

where m_k is defined in Equation (A8). The first six partial moments of the arcsine distribution ($k = 0, \dots, 5$) are depicted in Figure A1.

APPENDIX B: THE MOMENTS OF THE PURELY NONLINEAR OSCILLATOR

After lengthy calculations with the help of the software Mathematica™, the moments of ρ_{PNO}, described in Equation (89) can be obtained. It turns out that the integral can be represented in terms of the hypergeometric function, that is,

$$m_{\mathrm{PNO},k}(x) = \int_{-\infty}^{x} y^k \rho_{\mathrm{PNO}}(y)\mathrm{d}y = C(\alpha,A)\int_{-\infty}^{x} \frac{y^k}{\sqrt{A^{\alpha+1}-|y|^{\alpha+1}}}\mathrm{d}y = C(\alpha,A)\left.\frac{y^{k+1}\,{}_2F_1\left(\frac{1}{2},\frac{k+1}{\alpha+1};\frac{k+1}{\alpha+1}+1;\frac{|y|^{\alpha+1}}{A^{\alpha+1}}\right)}{(k+1)A^{\frac{\alpha+1}{2}}}\right|_{-A}^{x}, \tag{B1}$$

15214001, 0, Downloaded from https://onlinelibrary.wiley.com/doi/10.1002/zamm.202300432, Wiley Online Library on [23/03/2024]. See the Terms and Conditions (https://onlinelibrary.wiley.com/terms-and-conditions) on Wiley Online Library for rules of use; OA articles are governed by the applicable Creative Commons License

where ${}_2F_1$ is defined as

$$ {}_2F_1(a,b;c;z) := \frac{\Gamma(c)}{\Gamma(b)\Gamma(c-b)} \int_0^1 \frac{u^{b-1}(1-u)^{c-b-1}}{(1-uz)^a} \mathrm{d}u, \tag{B2} $$

and based on Equation (89), the constant $C(\alpha, A)$ is given by

$$ C(\alpha, A) := \frac{\alpha+1}{2\sqrt{\pi}} \frac{\Gamma\left(\frac{1}{2}+\frac{1}{\alpha+1}\right)}{\Gamma\left(\frac{1}{\alpha+1}\right)} A^{\frac{\alpha-1}{2}}. \tag{B3} $$

After the simplification of Equation (B1), the k^{th} partial moments of the purely nonlinear oscillator's motion are given by

$$ m_{\text{PNO},k}(x) = \frac{\alpha+1}{2\sqrt{\pi}A(k+1)} \frac{\Gamma\left(\frac{1}{2}+\frac{1}{\alpha+1}\right)}{\Gamma\left(\frac{1}{\alpha+1}\right)} \left(x^{k+1} {}_2F_1\left(\frac{1}{2}, \frac{k+1}{\alpha+1}; \frac{k+1}{\alpha+1}+1; \left(\frac{|x|}{A}\right)^{\alpha+1}\right) + (-1)^k A^{k+1} \sqrt{\pi} \frac{\Gamma\left(\frac{k+1}{\alpha+1}+1\right)}{\Gamma\left(\frac{k+1}{\alpha+1}+\frac{1}{2}\right)} \right). \tag{B4} $$

Evaluation of Equation (B4) at $x = A$ yields the k^{th} moment of the PNO's motion:

$$ m_{\text{PNO},k} = \begin{cases} \frac{\alpha+1}{k+1} \frac{\Gamma\left(\frac{1}{2}+\frac{1}{\alpha+1}\right)\Gamma\left(\frac{k+1}{\alpha+1}+1\right)}{\Gamma\left(\frac{1}{\alpha+1}\right)\Gamma\left(\frac{k+1}{\alpha+1}+\frac{1}{2}\right)} A^k & \text{for } k \text{ even}, \\ 0 & \text{for } k \text{ odd}. \end{cases} \tag{B5} $$

APPENDIX C: THE MOMENTS OF DUFFING-TYPE OSCILLATORS

The partial moments of the CPDs defined in Equations (92), (94), (98), (99) can be obtained by calculating

$$ m_{\text{DUFF},k}(x) = \int_{-\infty}^{x} y^k \rho_{\text{DUFF}}(y) \mathrm{d}y, \tag{C1} $$

where ρ_{DUFF} denotes any of the cases HDO, SDO, BDO_1, and BDO_2. After lengthy calculations with the help of the software Mathematica, it turns out that the integral is solvable for $V(x) < E_0 := c_1A^2/2 + c_3A^4/4$ in terms of the Appell hypergeometric function, that is,

$$ m_{\text{DUFF},k}(x) = C(c_1, c_3, A) \int_{x_a(c_1,c_3,E_0)}^{x} \frac{y^k}{\sqrt{2E_0 - c_1y^2 - c_3\frac{y^4}{2}}} \mathrm{d}y \tag{C2} $$

$$ = C(c_1, c_3, A) \frac{y^{k+1} F_1\left(\frac{k+1}{2}; \frac{1}{2}, \frac{1}{2}; \frac{k+3}{2}; \frac{c_3y^2}{\sqrt{c_1^2+4c_3E_0}-c_1}, -\frac{c_3y^2}{\sqrt{c_1^2+4c_3E_0}+c_1}\right)}{\sqrt{2E_0}(k+1)} \Bigg|_{x_a(c_1,c_3,E_0)}^{x} \quad \text{for } x_a(c_1,c_3,E_0) < x < x_b(c_1,c_3,E_0), \tag{C3} $$

with the constant $C(c_1, c_3, A)$ given by Equations (92), (94), (98) and (99), respectively, and with the lower turning point $x_a(c_1, c_3, E_0)$ and the upper turning point $x_b(c_1, c_3, E_0)$. The Appell hypergeometric function is defined as

$$ F_1(\alpha; \beta, \beta'; \gamma; x, y) = \frac{\Gamma(\gamma)}{\Gamma(\alpha)\Gamma(\gamma-\alpha)} \int_0^1 u^{\alpha-1}(1-u)^{\gamma-\alpha-1}(1-ux)^{-\beta}(1-uy)^{-\beta'} \mathrm{d}u. \tag{C4} $$

The turning points of the HDO and BDO_1 are

$$ x_{a,\text{HDO/BDO}_1} = -A = -\sqrt{\sqrt{\frac{c_1^2}{c_3^2} + \frac{4E_0}{c_3}} - \frac{c_1}{c_3}}, \quad \text{and} \quad x_{b,\text{HDO/BDO}_1} = A = \sqrt{\sqrt{\frac{c_1^2}{c_3^2} + \frac{4E_0}{c_3}} - \frac{c_1}{c_3}}. \tag{C5} $$

15214001, 0, Downloaded from https://onlinelibrary.wiley.com/doi/10.1002/zamm.202300432, Wiley Online Library on [23/03/2024]. See the Terms and Conditions (https://onlinelibrary.wiley.com/terms-and-conditions) on Wiley Online Library for rules of use; OA articles are governed by the applicable Creative Commons License

The turning point of SDO is

$$x_{a,\mathrm{SDO}} = -A = -\sqrt{-\frac{c_1}{c_3} - \sqrt{\frac{c_1^2}{c_3^2} + \frac{4E_0}{c_3}}}, \quad \text{and} \quad x_{b,\mathrm{SDO}} = A = \sqrt{-\frac{c_1}{c_3} - \sqrt{\frac{c_1^2}{c_3^2} + \frac{4E_0}{c_3}}}, \tag{C6}$$

while the turning points of BDO_2 are

$$x_{a,\mathrm{BDO}_2} = \sqrt{-\frac{c_1}{c_3} - \sqrt{\frac{c_1^2}{c_3^2} + \frac{4E_0}{c_3}}}, \quad \text{and} \quad x_{b,\mathrm{BDO}_2} = \sqrt{-\frac{c_1}{c_3} + \sqrt{\frac{c_1^2}{c_3^2} + \frac{4E_0}{c_3}}}. \tag{C7}$$

Since $\rho_{\mathrm{HDO}}(x)$ is even, its odd moments are all 0. Its even moments are

$$m_{\mathrm{HDO},k} = \frac{\sqrt{c_1 + c_3A^2}}{K\left(\frac{c_3A^2}{2(c_1+c_3A^2)}\right)} \frac{A^{k+1}F_1\left(\frac{k+1}{2}; \frac{1}{2}, \frac{1}{2}; \frac{k+3}{2}; 1, \frac{c_1^2}{2E_0c_3}\left(\sqrt{1+\frac{4E_0c_3}{c_1^2}} - 1\right) - 1\right)}{\sqrt{2E_0}(k+1)} \tag{C8}$$

$$= \frac{\sqrt{c_1 + c_3A^2}}{K\left(\frac{c_3A^2}{2(c_1+c_3A^2)}\right)} \frac{A^{k+1}\sqrt{\pi}\Gamma\left(\frac{k+3}{2}\right){}_2F_1\left(\frac{1}{2}, \frac{k+1}{2}; \frac{k}{2}+1; \frac{c_1^2}{2E_0c_3}\left(\sqrt{1+\frac{4E_0c_3}{c_1^2}} - 1\right) - 1\right)}{\Gamma\left(\frac{k}{2}+1\right)\sqrt{2E_0}(k+1)}. \tag{C9}$$

By the same argument, the odd moments of $\rho_{\mathrm{SDO}}(x)$ and $\rho_{\mathrm{BDO}_1}(x)$ are also all 0, and its even moments are given by

$$m_{\mathrm{SDO},k} = \frac{\sqrt{c_1 - |c_3|A^2}}{K\left(\frac{c_3A^2}{2(c_1-|c_3|A^2)}\right)} \frac{A^{k+1}\sqrt{\pi}\Gamma\left(\frac{k+3}{2}\right){}_2F_1\left(\frac{1}{2}, \frac{k+1}{2}; \frac{k}{2}+1; \frac{c_1^2}{2E_0|c_3|}\left(1 - \sqrt{1-\frac{4E_0|c_3|}{c_1^2}}\right) - 1\right)}{\Gamma\left(\frac{k}{2}+1\right)\sqrt{2E_0}(k+1)}, \tag{C10}$$

and

$$m_{\mathrm{BDO}_1,k} = \frac{\sqrt{c_3A^2 - |c_1|}}{K\left(\frac{c_3A^2}{2(c_3A^2-|c_1|)}\right)} \frac{A^{k+1}\sqrt{\pi}\Gamma\left(\frac{k+3}{2}\right){}_2F_1\left(\frac{1}{2}, \frac{k+1}{2}; \frac{k}{2}+1; -\frac{c_1^2}{2E_0c_3}\left(\sqrt{1+\frac{4E_0c_3}{c_1^2}} + 1\right) - 1\right)}{\Gamma\left(\frac{k}{2}+1\right)\sqrt{2E_0}(k+1)}. \tag{C11}$$

$\rho_{\mathrm{BDO}_2}(x)$ possesses exceptional characteristics as it exhibits asymmetry. The complexity of the distribution prevents us from presenting its moments in a closed form. Instead, we leave this task to the reader as an exercise.

APPENDIX D: CPD OF A BIHARMONIC FUNCTION WITH INCOMMENSURABLE FREQUENCIES

The following elliptic integral has to be solved to obtain an analytic value for the PDF of $g(t)$ given in Equation (107).

$$\rho_{\mathrm{BHO}}(x) = (\rho_1 * \rho_2)(x) = \int_{-\infty}^{\infty} \rho_1(\tau)\rho_2(x-\tau)\mathrm{d}\tau = \int_{-\infty}^{\infty} \frac{1}{\pi\sqrt{A_1^2 - \tau^2}} \mathbf{1}_{(-A_1,A_1)}(\tau) \frac{1}{\pi\sqrt{A_2^2 - (\tau - x)^2}} \mathbf{1}_{(-A_2+x,A_2+x)}(\tau)\mathrm{d}\tau, \tag{D1}$$

Without loss of generality, we assume that $A_1 \geq A_2$, and we introduce the polynomial

$$G(\tau) := \left(A_1^2 - \tau^2\right)\left(A_2^2 - (\tau - x)^2\right) \tag{D2}$$

with roots

$$\tau_1 = -A_1, \qquad \tau_2 = A_1, \qquad \tau_3 = x - A_2, \qquad \tau_4 = x + A_2. \tag{D3}$$

15214001, 0, Downloaded from https://onlinelibrary.wiley.com/doi/10.1002/zamm.202300432, Wiley Online Library on [23/03/2024]. See the Terms and Conditions (https://onlinelibrary.wiley.com/terms-and-conditions) on Wiley Online Library for rules of use; OA articles are governed by the applicable Creative Commons License

Thus, depending on the value of x integral (D1) can be reduced to

$$\rho_{\mathrm{BHO}}(x)=\begin{cases}0 & x<-A_1-A_2\\ \displaystyle\int_{-A_1}^{x+A_2} G^{-1/2}(\tau)\mathrm{d}\tau & -A_1-A_2<x<-A_1+A_2\\ \displaystyle\int_{x-A_2}^{x+A_2} G^{-1/2}(\tau)\mathrm{d}\tau & -A_1+A_2<x<A_1-A_2\\ \displaystyle\int_{x-A_2}^{A_1} G^{-1/2}(\tau)\mathrm{d}\tau & A_1-A_2<x<A_1+A_2\\ 0 & A_1+A_2<x\end{cases} \tag{D4}$$

The elliptic integral can be calculated by transforming Equation (D1) to Legendre's normal form [46] given as

$$\rho_{\mathrm{BHO}}(x;A_1,A_2)=C(x,A_1,A_2)\int_0^{\frac{\pi}{2}}\frac{\mathrm{d}\phi}{\sqrt{1-m(x,A_1,A_2)\sin^2\phi}}, \tag{D5}$$

where C and the parameter m are functions of the independent variable x and the parameters A_1 and A_2. To obtain the normal form in Equation (D5), the following rational transformation has to be applied.

$$\tau=\frac{a_3(a_2-a_4)-a_4(a_2-a_3)\sin^2\phi}{(a_2-a_4)-(a_2-a_3)\sin^2\phi}, \tag{D6}$$

where $a_1>a_2>a_3>a_4$ are the roots of $G(\tau)$, that is, the same values as $\tau_1,\ldots,\tau_4$, but in descending order. Substituting Equation (D6) in Equation (D4), we obtain

$$\rho_{\mathrm{BHO}}(x)=\begin{cases}0 & \text{for } x<-A_1-A_2,\\ \dfrac{1}{\pi^2\sqrt{A_1A_2}}K\left(\dfrac{(A_1+A_2)^2-x^2}{4A_1A_2}\right) & \text{for } -A_1-A_2<x<-A_1+A_2,\\ \dfrac{2}{\pi^2\sqrt{(A_1+A_2)^2-x^2}}K\left(\dfrac{4A_1A_2}{(A_1+A_2)^2-x^2}\right) & \text{for } -A_1+A_2<x<A_1-A_2,\\ \dfrac{1}{\pi^2\sqrt{A_1A_2}}K\left(\dfrac{(A_1+A_2)^2-x^2}{4A_1A_2}\right) & \text{for } A_1-A_2<x<A_1+A_2,\\ 0 & \text{for } A_1+A_2<x,\end{cases} \tag{D7}$$

where $K(m)$ is the complete elliptic integral of the first kind with modulus m.

15214001, 0, Downloaded from https://onlinelibrary.wiley.com/doi/10.1002/zamm.202300432, Wiley Online Library on [23/03/2024]. See the Terms and Conditions (https://onlinelibrary.wiley.com/terms-and-conditions) on Wiley Online Library for rules of use; OA articles are governed by the applicable Creative Commons License